THE KNOTTER

No.20 **NOVEMBER 1999.**

CONTENTS

A quarterly publication
for
the braiding artisan

Resale of this publication or copies thereof is strictly prohibited

This publication is available to braiding artisans only.

Copies may be obtained from:

A.G. Schaake,
21 Sundown Cresc.,
Hamilton,
New Zealand.

Solution to the Question in Issue No. 19

Question on pg. 422.

The string-run specification (22/5/22){123/312}12 under (1) is obviously impossible. This becomes immediately apparent when the numerals in the left periodic sequence 123 are provided with their ranking-numbers:

$n = 1$ for numeral $k = 1$, hence its ranking-number $j = |1 + 0|_3 = 1$.
$n = 2$ for numeral $k = 2$, hence its ranking-number $j = |2 + 2|_3 = 1$.
$n = 3$ for numeral $k = 3$, hence its ranking-number $j = |3 + (2 + 2)|_3 = 1$.

Hence we obtain for the left period the sequence $1_1 2_1 3_1$. But:
In a valid periodic sequence each ranking-number must occur once only.

In the previous issue of *The Braider* we have seen that the ranking-numbers j in the left periodic sequence range from $j = 1$ to $j = A_l$, and are calculated with the formula:

$$j = |n + \text{the sum of the first } (k-1) \text{ numerals of the left bight-boundary position specification}|_{A_l},$$

where A_l is the number of bights in a left period, and k is the n^{th} numeral in the left periodic sequence.

Furthermore we have seen that in the right periodic sequence the consecutive ranking-numbers j are $1, 2, 3, \cdots, A_r$.

Each numeral (bight-boundary number) in the left periodic sequence and in the right periodic sequence has furthermore a **complementary ranking-number** j_c.
In a valid periodic sequence each complementary ranking-number must occur once only.

In the left periodic sequence the consecutive complementary ranking-numbers j_c are $1, 2, 3, \cdots, A_l$, and in the right periodic sequence the complementary ranking-numbers j_c range from $j_c = 1$ to $j_c = A_r$, and are calculated with the formula:

$$j_c = |n - \text{the sum of the last } (k-1) \text{ numerals of the right bight-boundary position specification}|_{A_r},$$

where A_r is the number of bights in a right period, and k is the n^{th} numeral in the right periodic sequence.

From the conditions imposed on the ranking-numbers and complementary ranking-numbers it follows that the only valid left sequences for (1) are 132, 321 and 213, which with their ranking-numbers are respectively $1_1 3_3 2_2$, $3_2 2_1 1_3$ and $2_3 1_2 3_1$, while the only valid right sequences for (1) are 312, 123 and 231, which with their complementary ranking-numbers are respectively $3_3 1_2 2_1$, $1_1 2_3 3_2$ and $2_2 3_1 1_3$.

In a **set** of valid left sequences the consecutive A_l numerals in each of these sequences are always in an identical cyclic order; similarly in a set of valid right sequences the consecutive A_r numerals in each of these sequences are always in an identical cyclic order. In our example there is only one **set** of valid left sequences and there is only one **set** of valid right sequences.

Since any one left sequence of a **set** of **left** sequences can be associated with any one right sequence of a **set of right** sequences, we obtain a total of $A_l \cdot A_r$ left–right sequence **pairs** in each left–right **set** of sequence **pairs**. Thus if we have η_l left **sets** of valid left sequences and η_r right **sets** of valid right sequences, we have a total of $\eta_l \cdot \eta_r$ **sets** of left–right sequence **pairs**, and consequently we have a total of $\eta_l \cdot \eta_r \cdot A_l \cdot A_r$ left–right sequence **pairs**. In our example we have only one left sequence **set** ($\eta_l = 1$) and only one right sequence **set** ($\eta_r = 1$), and hence we have a total of $1 \cdot 1 = 1$ left–right

sequence **set** of left–right sequence **pairs**. Consequently we have a total of $1 \cdot 1 \cdot 3 \cdot 3 = 9$ left–right sequence **pairs**.

The stack of adjacent A^{**} different lower-left to upper-right half-cycles are read from their associated left–right sequence **pairs** as we have shown in the previous issue of *The Braider*.

Two left–right sequence pairs are identical when their respective stacks of adjacent A^{**} different lower-left to upper-right half-cycles are in cyclic order identical as far as the bight-boundary numbers are concerned. Note that the ranking-numbers play no role!!!

The number of different stacks (hence different cyclic adjacent sequences of lower-left to upper-right half-cycles and consequently different 'braid-types') associated with a **set** of left–right sequence **pairs** is equal to $d = \text{g.c.d.}(A_l, A_r)$. Hence the total number of different stacks (hence different cyclic adjacent sequences of lower-left to upper-right half-cycles and consequently different 'braid-types') associated with the total number of $\eta_l \cdot \eta_r$ **sets** of left–right sequence **pairs** is equal to $\eta_l \cdot \eta_r \cdot d$.

Thus in our example with $d = 3$, the number of different stacks of adjacent A^{**} lower-left to upper-right half-cycles for the single **set** ($\eta_l \cdot \eta_r = 1 \cdot 1 = 1$) of 9 ($A_l \cdot A_r = 3 \cdot 3 = 9$) left–right sequence **pairs** is equal to 3.

It will thus be obvious that in order to obtain the d different stacks of adjacent A^{**} lower-left to upper-right half-cycles for a **set** of left–right sequence pairs, we only have to obtain the stacks for the left–right sequence pairs in which the left sequence remains the same while the right sequence is respectively one of the first d consecutive cyclic ordered right sequences. Hence in our example for instance, we can obtain the 3 different stacks of the adjacent $A^{**} = 3$ lower-left to upper-right half-cycles from the 3 left–right sequence **pairs** for which the left sequence is 132 and the right sequence is successively 312, 123, 231. These left–right sequence pairs give us the following 3 different stacks of adjacent lower-left to upper-right half-cycles:

$1 \longrightarrow 3$	$1 \longrightarrow 1$	$1 \longrightarrow 2$
$3 \longrightarrow 1$	$3 \longrightarrow 2$	$3 \longrightarrow 3$
$2 \longrightarrow 2$	$2 \longrightarrow 3$	$2 \longrightarrow 1$

Although the ranking-numbers do not play a role here, we normally leave them, at least initially, attached to the bight-boundary numbers. The reason for this is readily demonstrated with the sequence **set** 1123/113142 of the $A_l \cdot A_r = 4 \cdot 6 = 24$ left–right sequence pairs of the example in the previous issue of *The Braider* on pg.420. The 2 different stacks of adjacent lower-left to upper-right half-cycles are:

$1_1 \longrightarrow 1_1$	$1_1 \longrightarrow 1_1$
$1_2 \longrightarrow 1_2$	$1_2 \longrightarrow 3_2$
$2_4 \longrightarrow 3_3$	$2_4 \longrightarrow 1_3$
$3_3 \longrightarrow 1_4$	$3_3 \longrightarrow 4_4$
$1_1 \longrightarrow 4_5$	$1_1 \longrightarrow 2_5$
$1_2 \longrightarrow 2_6$	$1_2 \longrightarrow 1_6$
$2_4 \longrightarrow 1_1$	$2_4 \longrightarrow 1_1$
$3_3 \longrightarrow 1_2$	$3_3 \longrightarrow 3_2$
$1_1 \longrightarrow 3_3$	$1_1 \longrightarrow 1_3$
$1_2 \longrightarrow 1_4$	$1_2 \longrightarrow 4_4$
$2_4 \longrightarrow 4_5$	$2_4 \longrightarrow 2_5$
$3_3 \longrightarrow 2_6$	$3_3 \longrightarrow 1_6$

Since $A_l = 4$ and $A_r = 6$, we obtain $d = \text{g.c.d.}(A_l, A_r) = 2$. Thus for this **set** of left–right sequence pairs we obtain 2 different stacks of $A^{**} = 12$ adjacent lower-left to upper-right half-cycles. These $d = 2$ different stacks may be obtained from the 2 left–right sequence pairs in which the left sequence is $1_1 1_2 2_4 3_3$ and the right sequence is respectively one of the first $d = 2$ consecutive cyclic ordered right sequences, hence respectively $1_1 1_2 3_3 1_4 4_5 2_6$ and $1_1 3_2 1_3 4_4 2_5 1_6$. Note their respective ranking-numbers!!!

After leaving the ranking-numbers off, we obtain:

$1 \longrightarrow 1$	$1 \longrightarrow 1$
$1 \longrightarrow 1$	$1 \longrightarrow 3$
$2 \longrightarrow 3$	$2 \longrightarrow 1$
$3 \longrightarrow 1$	$3 \longrightarrow 4$
$1 \longrightarrow 4$	$1 \longrightarrow 2$
$1 \longrightarrow 2$	$1 \longrightarrow 1$
$2 \longrightarrow 1$	$2 \longrightarrow 1$
$3 \longrightarrow 1$	$3 \longrightarrow 3$
$1 \longrightarrow 3$	$1 \longrightarrow 1$
$1 \longrightarrow 1$	$1 \longrightarrow 4$
$2 \longrightarrow 4$	$2 \longrightarrow 2$
$3 \longrightarrow 2$	$3 \longrightarrow 1$

The valid **left** sequence **sets** (the valid left cyclic sequences of k-values) are determined by the **left** bight-boundary position specification, and similarly the valid **right** sequence **sets** (the valid right cyclic sequences of k-values) are determined by the **right** bight-boundary position specification. These valid sequence **sets** of k-values can readily be obtained by means of the calculation procedure set out in Fig. 362 for $(12/**/113)\{****/******\}$ as an Example.

To a valid sequence **set**, each row **must** contribute only one column-cell containing a k-value and in a valid sequence **set**, **each** k-value **must** at least be present once.

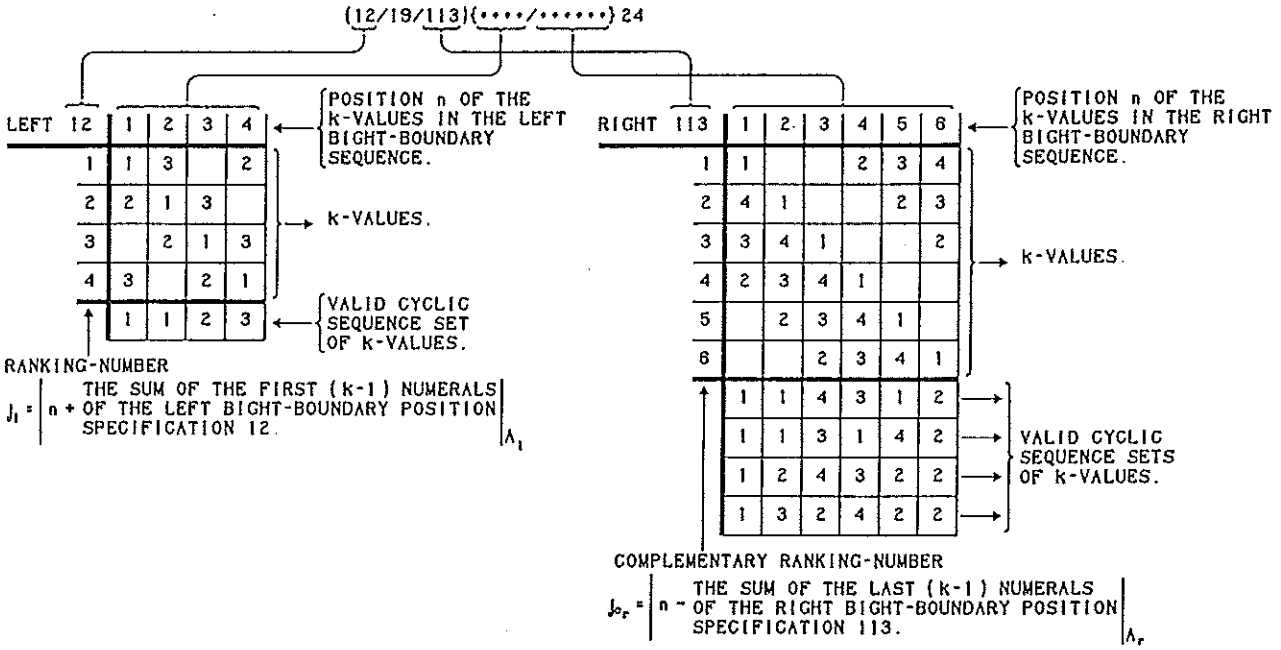

Fig. 362 — An Example calculation procedure for the valid sequence **sets**.

When there is on **left** bight-boundary 1 a Standing End (and hence its associated Working End), we take by convention for a **left** sequence always one which begins with

bight-boundary 1. Although we could obviously begin with another bight-boundary, this convention ensures that the RRHC† always starts at left bight-boundary 1, and that the LRHC† has the ranking-number 1 for its left-hand bight-point.

In the Example of Fig. 362, the **left** bight-boundary position specification 12 determines that there is only one valid **left** sequence **set** with $A_l = 4$ k-values ($1 \leq k \leq \mathcal{K}_l$, hence $1 \leq k \leq 3$), while the **right** bight-boundary position specification 113 determines that there are four valid **right** sequence **sets** with $A_r = 6$ k-values ($1 \leq k \leq \mathcal{K}_r$, hence $1 \leq k \leq 4$). Thus, these left and right bight-boundary position specifications determine that there are with $A_l = 4$ and $A_r = 6$ a total of $1 \times 4 \times d = 1 \times 4 \times 2 = 8$ different stacks of adjacent lower-left to upper-right half-cycles possible, which means that there are a total of 8 different 'braid-types' possible.

For the bight-boundary position specifications of sub-questions (1), (2) and (3), the calculations for the valid left and right sequence **sets** of k-values are shown in Fig. 363.

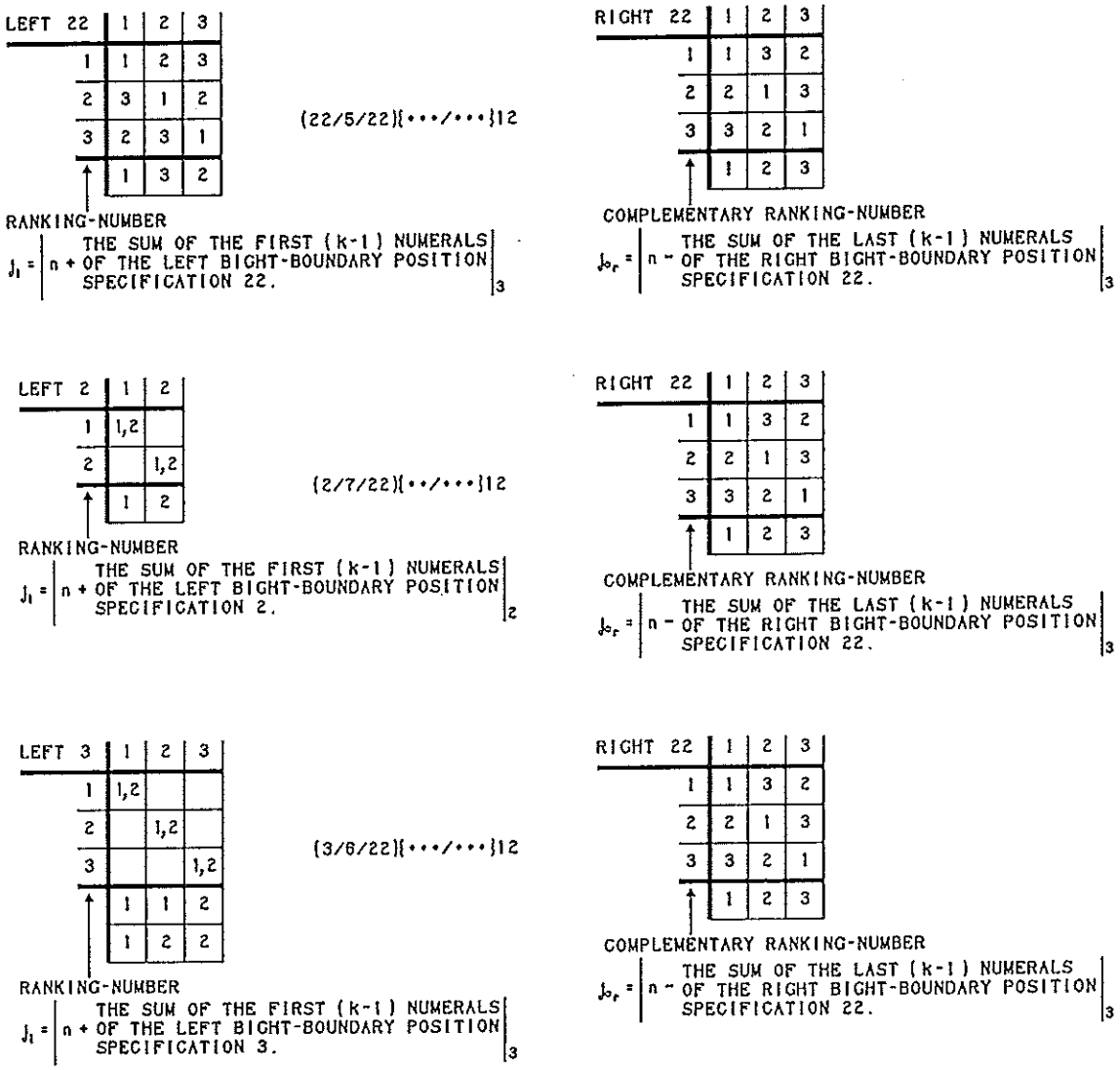

Fig. 363 — The calculations for the valid sequence **sets** associated with the sub-questions (1), (2), (3).

† See previous Issue of *The Braider*, No. 19, pp. 415 & 416.

For the bight-boundary position specifications in sub-question (1) we obtain the one valid left sequence **set** ($\eta_l = 1$) and the one valid right sequence **set** ($\eta_r = 1$) which give the sequences discussed on pg. 437. Since $d = 3$, we thus obtain three different stacks of adjacent lower-left to upper-right half-cycles ($\eta_l \cdot \eta_r \cdot d = 1 \cdot 1 \cdot 3 = 3$). Each such stack consists of three adjacent lower-left to upper-right half-cycles ($A^{**} = 3$). Refer to pg. 438.

For the bight-boundary position specifications in sub-question (2) we obtain the one valid left sequence **set** ($\eta_l = 1$) and the one valid right sequence **set** ($\eta_r = 1$). Since $d = 1$, we thus obtain only one stack of adjacent lower-left to upper-right half-cycles ($\eta_l \cdot \eta_r \cdot d = 1 \cdot 1 \cdot 1 = 1$). The stack consists of six adjacent lower-left to upper-right half-cycles ($A^{**} = 6$).

For the bight-boundary position specifications in sub-question (3) we obtain the two valid left sequence **sets** ($\eta_l = 2$) and the one valid right sequence **set** ($\eta_r = 1$). Since $d = 3$, we thus obtain six different stacks of adjacent lower-left to upper-right half-cycles ($\eta_l \cdot \eta_r \cdot d = 2 \cdot 1 \cdot 3 = 6$). Each such stack consists of three adjacent lower-left to upper-right half-cycles ($A^{**} = 3$).

Thus for the bight-boundary position specification (22/5/22) in sub-question (1), we have the following three different string-run specifications:

(1a). $(22/5/22)\{132/123\}12$.
(1b). $(22/5/22)\{132/231\}12$.
(1c). $(22/5/22)\{132/312\}12$.

(1a):

The stack of adjacent lower-left to upper-right half-cycles for the string-run specification $(22/5/22)\{1_1 3_3 2_2 / 1_1 2_2 3_3\}12$ is:

$$1_1 \longrightarrow 1_1$$
$$3_3 \longrightarrow 2_2$$
$$2_2 \longrightarrow 3_3$$

For the first-return string-runs we thus obtain:

1_1
$\nwarrow 2_2$
$3_3 \nwarrow 3_3$
$2_2 \nwarrow 1_1$
1_1

$$l_{1_{j_l}} = 1_1 \longrightarrow 1_1 = r_{1_{j_r}} \rightarrow j'_l = |1+4+5+4|_3 = 2 \rightarrow l_{2_{j'_l}} = 2_2 .$$
$$l_{2_{j'_l}} = 2_2 \longleftarrow 1_1 = r_{1_{j_r}} \rightarrow j'_r = |1+4+5+2|_3 = 3 \rightarrow r_{2_{j'_r}} = 3_3 .$$
$$l_{2_{j_l}} = 2_2 \longrightarrow 3_3 = r_{2_{j_r}} \rightarrow j'_l = |2+2+5+0|_3 = 3 \rightarrow l_{3_{j'_l}} = 3_3 .$$
$$l_{3_{j'_l}} = 3_3 \longleftarrow 3_3 = r_{2_{j_r}} \rightarrow j'_r = |3+0+5+0|_3 = 2 \rightarrow r_{3_{j'_r}} = 2_2 .$$
$$l_{3_{j_l}} = 3_3 \longrightarrow 2_2 = r_{3_{j_r}} \rightarrow j'_l = |3+0+5+2|_3 = 1 \rightarrow l_{4_{j'_l}} = 1_1 .$$
$$l_{4_{j'_l}} = 1_1 \longleftarrow 2_2 = r_{3_{j_r}} \rightarrow j'_r = |2+2+5+4|_3 = 1 \rightarrow r_{4_{j'_r}} = 1_1 .$$

$$P_c = \frac{\alpha \cdot x + \sum(\Delta_{l_i} + \Delta_{r_i})}{A^{**}} = \frac{3 \cdot 5 + (4+2+0) + (4+0+2)}{3} = 9 .$$

$$\text{g.c.d.}\,(P_c\,,\, B^{**}) = \text{g.c.d.}\,(9\,,\, 4) = 1 .$$

Hence:

$$P_{total} = \sum P_{component} = 9 .$$

$$\left.\begin{matrix}\text{number of}\\ \text{components}\end{matrix}\right\} = \text{number of first-return string-runs} = 1\,.$$

$$\left.\begin{matrix}\text{total number of}\\ \text{essential strings}\end{matrix}\right\} = \sum \text{sub-components} = 1\,.$$

(1b):

The stack of adjacent lower-left to upper-right half-cycles for the string-run specification $(22/5/22)\{1_1 3_3 2_2/2_1 3_2 1_3\}12$ is:

$$\begin{aligned} 1_1 &\longrightarrow 2_1\\ 3_3 &\longrightarrow 3_2\\ 2_2 &\longrightarrow 1_3 \end{aligned}$$

For the first-return string-runs we thus obtain:

$1_1 \nwarrow 1_3 \nearrow 2_2 \nwarrow 3_2 \nearrow 3_3 \nwarrow 2_1 \nearrow 1_1$

$$\begin{aligned}
l_{1_{j_l}} = 1_1 \longrightarrow 2_1 = r_{1_{j_r}} &\rightarrow j'_l = |1+4+5+2|_3 = 3 \rightarrow l_{2_{j'_l}} = 3_3\,.\\
l_{2_{j'_l}} = 3_3 \longleftarrow 2_1 = r_{1_{j_r}} &\rightarrow j'_r = |1+2+5+0|_3 = 2 \rightarrow r_{2_{j'_r}} = 3_2\,.\\
l_{2_{j_l}} = 3_3 \longrightarrow 3_2 = r_{2_{j_r}} &\rightarrow j'_l = |3+0+5+0|_3 = 2 \rightarrow l_{3_{j'_l}} = 2_2\,.\\
l_{3_{j'_l}} = 2_2 \longleftarrow 3_2 = r_{2_{j_r}} &\rightarrow j'_r = |2+0+5+2|_3 = 3 \rightarrow r_{3_{j'_r}} = 1_3\,.\\
l_{3_{j_l}} = 2_2 \longrightarrow 1_3 = r_{3_{j_r}} &\rightarrow j'_l = |2+2+5+4|_3 = 1 \rightarrow l_{4_{j'_l}} = 1_1\,.\\
l_{4_{j'_l}} = 1_1 \longleftarrow 1_3 = r_{3_{j_r}} &\rightarrow j'_r = |3+4+5+4|_3 = 1 \rightarrow r_{4_{j'_r}} = 2_1\,.
\end{aligned}$$

$$P_c = \frac{\alpha\cdot x + \sum(\Delta_{l_i}+\Delta_{r_i})}{A^{**}} = \frac{3\cdot 5+(4+0+2)+(2+0+4)}{3} = 9\,.$$

$\text{g.c.d.}\,(P_c\,,\,B^{**}) = \text{g.c.d.}\,(9\,,\,4) = 1\,.$

Hence:

$$P_{total} = \sum P_{component} = 9\,.$$

$$\left.\begin{matrix}\text{number of}\\ \text{components}\end{matrix}\right\} = \text{number of first-return string-runs} = 1\,.$$

$$\left.\begin{matrix}\text{total number of}\\ \text{essential strings}\end{matrix}\right\} = \sum \text{sub-components} = 1\,.$$

(1c):

The stack of adjacent lower-left to upper-right half-cycles for the string-run specification $(22/5/22)\{1_1 3_3 2_2/3_1 1_2 2_3\}12$ is:

$$\begin{aligned} 1_1 &\longrightarrow 3_1\\ 3_3 &\longrightarrow 1_2\\ 2_2 &\longrightarrow 2_3 \end{aligned}$$

For the first-return string-runs we thus obtain:

$1_1 \nwarrow 3_1 \nearrow 1_1$

$$\begin{aligned}
l_{1_{j_l}} = 1_1 \longrightarrow 3_1 = r_{1_{j_r}} &\rightarrow j'_l = |1+4+5+0|_3 = 1 \rightarrow l_{2_{j'_l}} = 1_1\,.\\
l_{2_{j'_l}} = 1_1 \longleftarrow 3_1 = r_{1_{j_r}} &\rightarrow j'_r = |1+0+5+4|_3 = 1 \rightarrow r_{2_{j'_r}} = 3_1\,.
\end{aligned}$$

$P_{c_1} = \frac{\alpha \cdot x + \sum(\Delta_{l_i} + \Delta_{r_i})}{A^{**}} = \frac{1 \cdot 5 + (4) + (0)}{3} = 3\,.$
g.c.d. $(P_{c_1}\,,\, B^{**}) =$ g.c.d. $(3\,,\, 4) = 1\,.$

$3_3 \nwarrow 1_2 \nearrow 3_3$

$l_{1_{j_l}} = 3_3 \longrightarrow 1_2 = r_{1_{j_r}} \;\rightarrow\; j'_l = |3+0+5+4|_3 = 3 \;\rightarrow\; l_{2_{j'_l}} = 3_3\,.$
$l_{2_{j'_l}} = 3_3 \longleftarrow 1_2 = r_{1_{j_r}} \;\rightarrow\; j'_r = |2+4+5+0|_3 = 2 \;\rightarrow\; r_{2_{j'_r}} = 1_2\,.$

$P_{c_2} = \frac{\alpha \cdot x + \sum(\Delta_{l_i} + \Delta_{r_i})}{A^{**}} = \frac{1 \cdot 5 + (0) + (4)}{3} = 3\,.$
g.c.d. $(P_{c_2}\,,\, B^{**}) =$ g.c.d. $(3\,,\, 4) = 1\,.$

$2_2 \nwarrow 2_3 \nearrow 2_2$

$l_{1_{j_l}} = 2_2 \longrightarrow 2_3 = r_{1_{j_r}} \;\rightarrow\; j'_l = |2+2+5+2|_3 = 2 \;\rightarrow\; l_{2_{j'_l}} = 2_2\,.$
$l_{2_{j'_l}} = 2_2 \longleftarrow 2_3 = r_{1_{j_r}} \;\rightarrow\; j'_r = |3+2+5+2|_3 = 3 \;\rightarrow\; r_{2_{j'_r}} = 2_3\,.$

$P_{c_3} = \frac{\alpha \cdot x + \sum(\Delta_{l_i} + \Delta_{r_i})}{A^{**}} = \frac{1 \cdot 5 + (2) + (2)}{3} = 3\,.$
g.c.d. $(P_{c_3}\,,\, B^{**}) =$ g.c.d. $(3\,,\, 4) = 1\,.$

Hence:

$$P_{total} = \sum P_{component} = 3 + 3 + 3 = 9\,.$$

number of components $\Big\}$ = number of first-return string-runs $= 1 + 1 + 1 = 3\,.$

total number of essential strings $\Big\}$ $= \sum$ sub-components $= 1 + 1 + 1 = 3\,.$

The string-run diagram of $(22/5/22)\{132/312\}12$ is shown at the left in Fig. 364.

With the convention discussed on pp. 439 and 440, there are no alternative string-run specifications to the ones given above for (1a), (1b) and (1c).

Sub-question (2):

The stack of adjacent lower-left to upper-right half-cycles for the string-run specification $(2/7/22)\{1_1 2_2 / 3_1 1_2 2_3\}12$ is:

$$1_1 \longrightarrow 3_1$$
$$2_2 \longrightarrow 1_2$$
$$1_1 \longrightarrow 2_3$$
$$2_2 \longrightarrow 3_1$$
$$1_1 \longrightarrow 1_2$$
$$2_2 \longrightarrow 2_3$$

For the first-return string-runs we thus obtain:

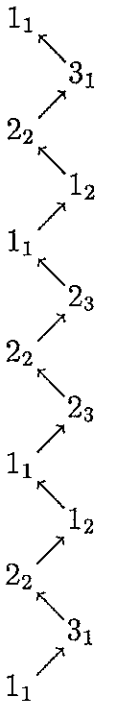

$$
\begin{array}{llll}
l_{1_{j_l}} = 1_1 \longrightarrow 3_1 = r_{1_{j_r}} & \rightarrow & j'_l = |1+2+7+0|_2 = 2 & \rightarrow \quad l_{2_{j'_l}} = 2_2 \,. \\
l_{2_{j'_l}} = 2_2 \longleftarrow 3_1 = r_{1_{j_r}} & \rightarrow & j'_r = |1+0+7+0|_3 = 2 & \rightarrow \quad r_{2_{j'_r}} = 1_2 \,. \\
l_{2_{j_l}} = 2_2 \longrightarrow 1_2 = r_{2_{j_r}} & \rightarrow & j'_l = |2+0+7+4|_2 = 1 & \rightarrow \quad l_{3_{j'_l}} = 1_1 \,. \\
l_{3_{j'_l}} = 1_1 \longleftarrow 1_2 = r_{2_{j_r}} & \rightarrow & j'_r = |2+4+7+2|_3 = 3 & \rightarrow \quad r_{3_{j'_r}} = 2_3 \,. \\
l_{3_{j_l}} = 1_1 \longrightarrow 2_3 = r_{3_{j_r}} & \rightarrow & j'_l = |1+2+7+2|_2 = 2 & \rightarrow \quad l_{4_{j'_l}} = 2_2 \,. \\
l_{4_{j'_l}} = 2_2 \longleftarrow 2_3 = r_{3_{j_r}} & \rightarrow & j'_r = |3+2+7+0|_3 = 3 & \rightarrow \quad r_{4_{j'_r}} = 2_3 \,. \\
l_{4_{j_l}} = 2_2 \longrightarrow 2_3 = r_{4_{j_r}} & \rightarrow & j'_l = |2+0+7+2|_2 = 1 & \rightarrow \quad l_{5_{j'_l}} = 1_1 \,. \\
l_{5_{j'_l}} = 1_1 \longleftarrow 2_3 = r_{4_{j_r}} & \rightarrow & j'_r = |3+2+7+2|_3 = 2 & \rightarrow \quad r_{5_{j'_r}} = 1_2 \,. \\
l_{5_{j_l}} = 1_1 \longrightarrow 1_2 = r_{5_{j_r}} & \rightarrow & j'_l = |1+2+7+4|_2 = 2 & \rightarrow \quad l_{6_{j'_l}} = 2_2 \,. \\
l_{6_{j'_l}} = 2_2 \longleftarrow 1_2 = r_{5_{j_r}} & \rightarrow & j'_r = |2+4+7+0|_3 = 1 & \rightarrow \quad r_{6_{j'_r}} = 3_1 \,. \\
l_{6_{j_l}} = 2_2 \longrightarrow 3_1 = r_{6_{j_r}} & \rightarrow & j'_l = |2+0+7+0|_2 = 1 & \rightarrow \quad l_{7_{j'_l}} = 1_1 \,. \\
l_{7_{j'_l}} = 1_1 \longleftarrow 3_1 = r_{6_{j_r}} & \rightarrow & j'_r = |1+0+7+2|_3 = 1 & \rightarrow \quad r_{7_{j'_r}} = 3_1 \,.
\end{array}
$$

$$P_c = \frac{\alpha \cdot x + \sum(\Delta_{l_i} + \Delta_{r_i})}{A^{**}} = \frac{6 \cdot 7 + (2+0+2+0+2+0) + (0+4+2+2+4+0)}{6} = 10 \,.$$

$$\text{g.c.d.}\,(P_c\,,\, B^{**}) = \text{g.c.d.}\,(10\,,\, 2) = 2 \,.$$

Hence:

$$P_{total} = \sum P_{component} = 10 \,.$$

$$\left.\begin{matrix}\text{number of} \\ \text{components}\end{matrix}\right\} = \text{number of first-return string-runs} = 1 \,.$$

$$\left.\begin{matrix}\text{total number of} \\ \text{essential strings}\end{matrix}\right\} = \sum \text{sub-components} = 2 \,.$$

The string-run diagram of $(2/7/22)\{12/312\}12$ is shown at the centre in Fig. 364.

With the convention discussed on pp. 439 and 440, there are two alternative string-run specifications for the string-run specification $(2/7/22)\{12/312\}12$:

$$(2/7/22)\{12/123\}12 \,.$$
$$(2/7/22)\{12/231\}12 \,.$$

Sub-question (3):

The stack of adjacent lower-left to upper-right half-cycles for the string-run specification $(3/6/22)\{1_1 1_2 2_3/3_1 1_2 2_3\}12$ is:

$$1_1 \longrightarrow 3_1$$
$$1_2 \longrightarrow 1_2$$
$$2_3 \longrightarrow 2_3$$

For the first-return string-runs we thus obtain:

$$\begin{array}{l} 1_1 \\ \quad\nwarrow \\ \quad\quad 3_1 \\ \quad\nearrow \\ 1_1 \end{array} \qquad \begin{array}{llll} l_{1_{j_l}} = 1_1 \longrightarrow 3_1 = r_{1_{j_r}} & \rightarrow & j_l' = |1+3+6+0|_3 = 1 & \rightarrow \quad l_{2_{j_l'}} = 1_1 . \\ l_{2_{j_l'}} = 1_1 \longleftarrow 3_1 = r_{1_{j_r}} & \rightarrow & j_r' = |1+0+6+3|_3 = 1 & \rightarrow \quad r_{2_{j_r'}} = 3_1 . \end{array}$$

$$P_{c_1} = \frac{\alpha \cdot x + \sum(\Delta_{l_i} + \Delta_{r_i})}{A^{**}} = \frac{1 \cdot 6 + (3) + (0)}{3} = 3 .$$

$$\text{g.c.d.}\,(P_{c_1}\,,\, B^{**}) = \text{g.c.d.}\,(3\,,\,4) = 1 .$$

$$\begin{array}{l} 1_2 \\ \quad\nwarrow \\ \quad\quad 2_3 \\ \quad\nearrow \\ 2_3 \\ \quad\nwarrow \\ \quad\quad 1_2 \\ \quad\nearrow \\ 1_2 \end{array} \qquad \begin{array}{llll} l_{1_{j_l}} = 1_2 \longrightarrow 1_2 = r_{1_{j_r}} & \rightarrow & j_l' = |2+3+6+4|_3 = 3 & \rightarrow \quad l_{2_{j_l'}} = 2_3 . \\ l_{2_{j_l'}} = 2_3 \longleftarrow 1_2 = r_{1_{j_r}} & \rightarrow & j_r' = |2+4+6+0|_3 = 3 & \rightarrow \quad r_{2_{j_r'}} = 2_3 . \\ l_{1_{j_l}} = 2_3 \longrightarrow 2_3 = r_{1_{j_r}} & \rightarrow & j_l' = |3+0+6+2|_3 = 2 & \rightarrow \quad l_{2_{j_l'}} = 1_2 . \\ l_{2_{j_l'}} = 1_2 \longleftarrow 2_3 = r_{1_{j_r}} & \rightarrow & j_r' = |3+2+6+3|_3 = 2 & \rightarrow \quad r_{2_{j_r'}} = 1_2 . \end{array}$$

$$P_{c_2} = \frac{\alpha \cdot x + \sum(\Delta_{l_i} + \Delta_{r_i})}{A^{**}} = \frac{2 \cdot 6 + (3+0) + (4+2)}{3} = 7 .$$

$$\text{g.c.d.}\,(P_{c_2}\,,\, B^{**}) = \text{g.c.d.}\,(7\,,\,4) = 1 .$$

Hence:

$$P_{total} = \sum P_{component} = 3 + 7 = 10 .$$

$$\left.\begin{array}{r}\text{number of} \\ \text{components}\end{array}\right\} = \text{number of first-return string-runs} = 1 + 1 = 2 .$$

$$\left.\begin{array}{r}\text{total number of} \\ \text{essential strings}\end{array}\right\} = \sum \text{sub-components} = 1 + 1 = 2 .$$

The string-run diagram of $(3/6/22)\{112/312\}12$ is shown at the right in Fig. 364.

With the convention discussed on pp. 439 and 440, there is one alternative string-run specifications for the string-run specification $(3/6/22)\{112/312\}12$:

$$(3/6/22)\{121/123\}12 .$$

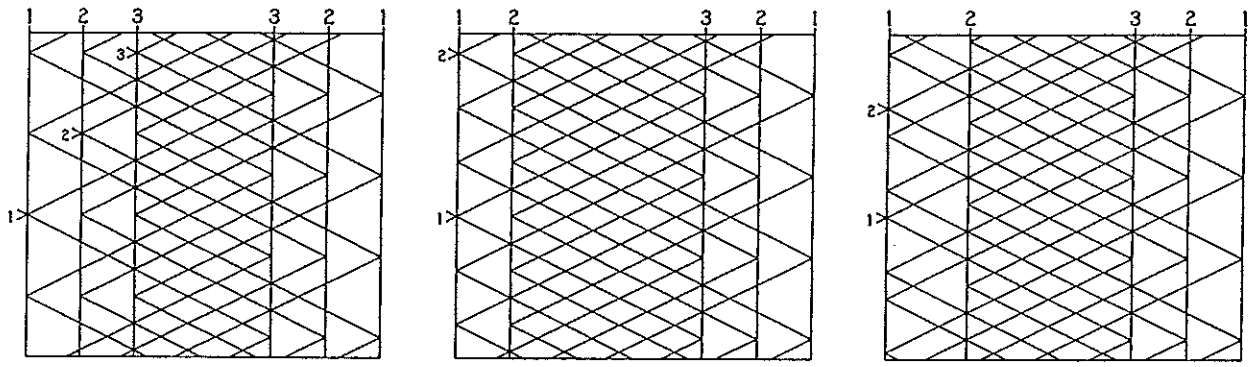

Fig. 364 — The string-run diagrams of (1c), (2), (3).

Scenes from the Knot Universe

In Issue No. 18 of *The Braider*, pg. 403, we mentioned that any attempt in creating a knot-classification system constitutes a futile exercise, an exercise that can only be contemplated by those who haven't got the faintest idea of what knots are really about. In this article we shall show that knots with even a very simple string-run layout are not easy to classify completely. We shall therefore not make any attempt to even partly classify the knots discussed, but rather show some relationships instead.

Relationships between knots are solely governed by their grid-diagrams and not by tying procedures, superficial appearances or behavioural aspects.

A grid-diagram consists of two important aspects: (1) the string-run and (2) the coding which is superimposed upon the string-run. The most basic aspect is the string-run. The coding may enable the string-run to be rearranged, which will then result in further relationships. It is therefore important to stress that such rearrangements do never furnish equivalent knots or braids.† A few simple examples are depicted in Fig. 365. The right-hand grid-diagram in the uppermost example is not a rearrangement of the left-hand grid-diagram since the left-hand grid-diagram cannot be rearranged into the right-hand grid-diagram without causing a full turn in the string with a left helix. In the next example, the two interbraided knots can be slid apart and hence the two right-hand grid-diagrams are a rearrangement of the left-hand grid-diagram. In the lowermost example the two right-hand grid-diagrams are not a rearrangement of the left-hand grid-diagram since such a rearrangement is impossible to accomplish.

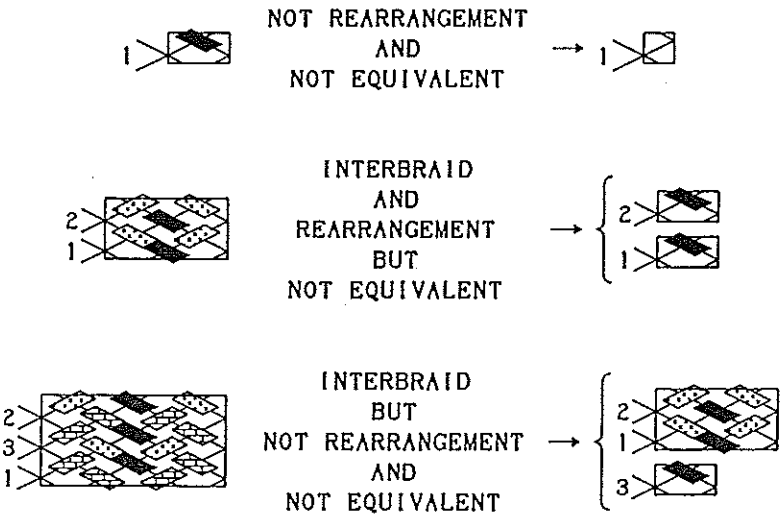

Fig. 365 — A few simple Examples.

The string-run layout we shall concern ourselves with is depicted at the left in Fig. 366; it is an interbraid of two components with equivalent string-runs. This string-run layout can be depicted for example by each of the two string-run diagrams to its right. The central string-run diagram is that of a flat braid, whereas the rightmost string-run diagram is that of its cylindrical form. The **everted** string-run layout and the two everted string-run diagrams associated with the string-runs in Fig. 366 are depicted in Fig. 367.

It should be stressed here that by everting a knot we obtain in general a different knot (refer for more details to Pamphlet No. 8: *Knots — Facts and Fallacies*).

† The topological knot theory goes also here totally astray.

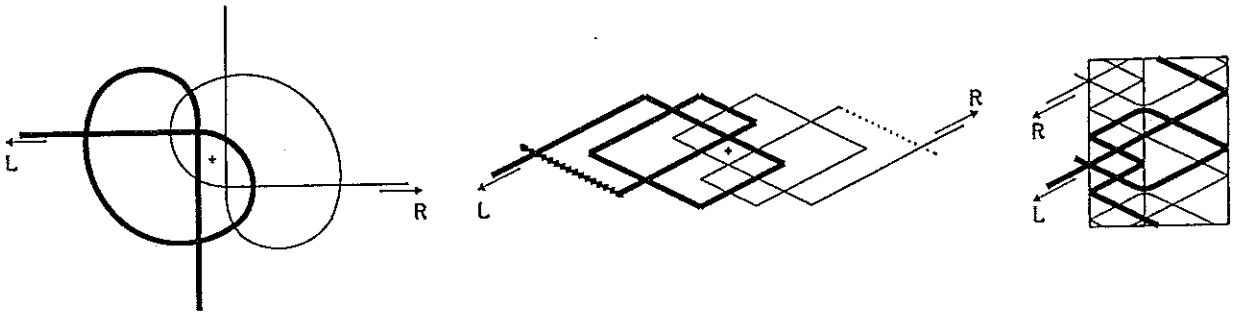

Fig. 366 — The string-run layout to be discussed.

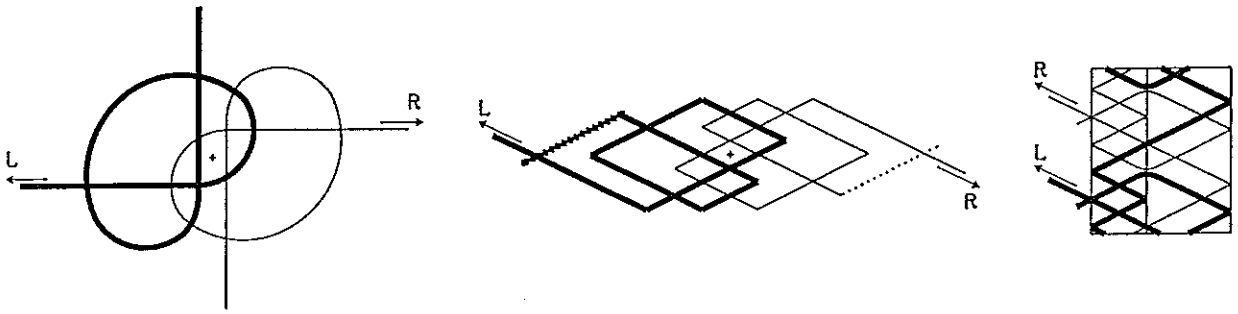

Fig. 367 — The everted string-run layout and everted string-run diagrams of Fig. 366.

For the superimposed coding in the upper-left diagram of Fig. 368, the upper-right diagram of its cylindrical form can be rearranged into the diagram of the cylindrical braid immediately below it. Furthermore, since we can lift in the upper-left diagram the two dotted string-parts up and slide the left-hand string-part to the right while sliding the right-hand string-part to the left, we can rearrange the upper-left string-run diagram with its superimposed coding into the diagram immediately below it. The cylindrical form of this diagram is depicted to its right. In turn this diagram can again be rearranged into the string-run diagram of the cylindrical braid immediately below it.

Similarly, for the superimposed coding in the leftmost third diagram from the top in Fig. 368, the diagram of its cylindrical form (depicted on its right) can be rearranged into the string-run diagram of the cylindrical braid immediately below it. In this case we drop the two dotted string-parts and slide the left-hand string-part to the right while sliding the right-hand string-part to the left.

The codings indicated in Fig. 369 enable us to slide the two central SW-NE running string-parts past each other in the SE-NW direction.This results in the lowermost rearranged string-run diagrams.

We shall limit our discussion not only to string material that is symmetric with respect to shape, colour and pattern/texture, but also to the string-run diagrams depicted in Figs. 368 & 369, except in one case where a further string-run layout, depicted by the two lowermost string-run diagrams in Fig. 370, will be considered (see pg. 457). This string-run layout can be obtained from the lowermost string-run diagrams in Fig. 369 by the codings indicated in Fig. 370. We shall furthermore limit our discussion to coding arrangements which are **balanced**† and in which each of the two interbraided components are 'overhand' knots.

† These are the coding arrangements in which the crossing-sequences from the ends L and R are either identical or opposites for each of the two interbraided strings.

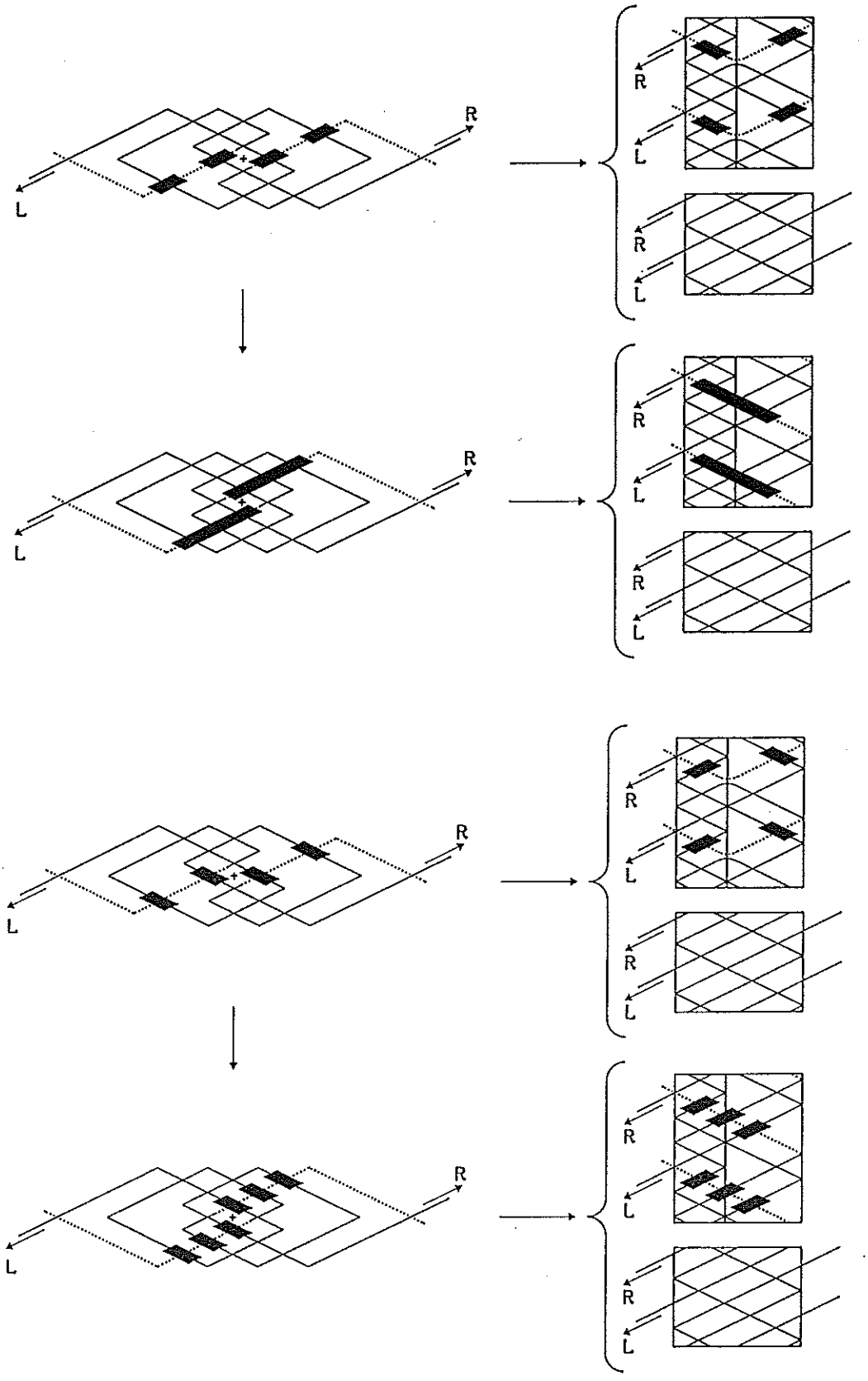

Fig. 368 — Some rearrangements facilitated by the indicated superimposed coding.

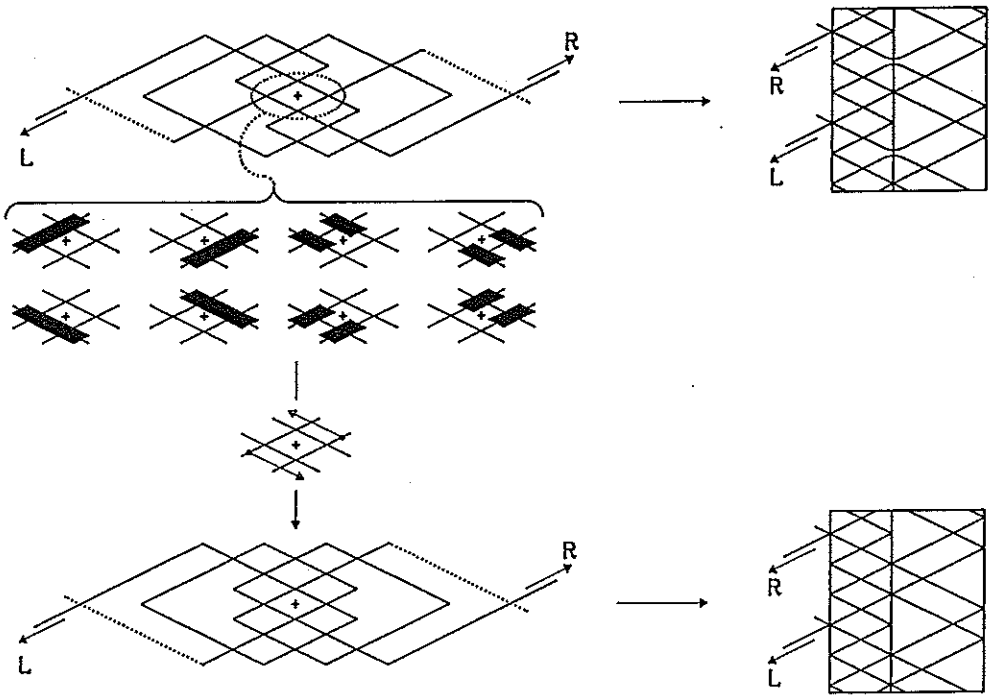

Fig. 369 — Further codings which facilitate a rearrangement of the string-run.

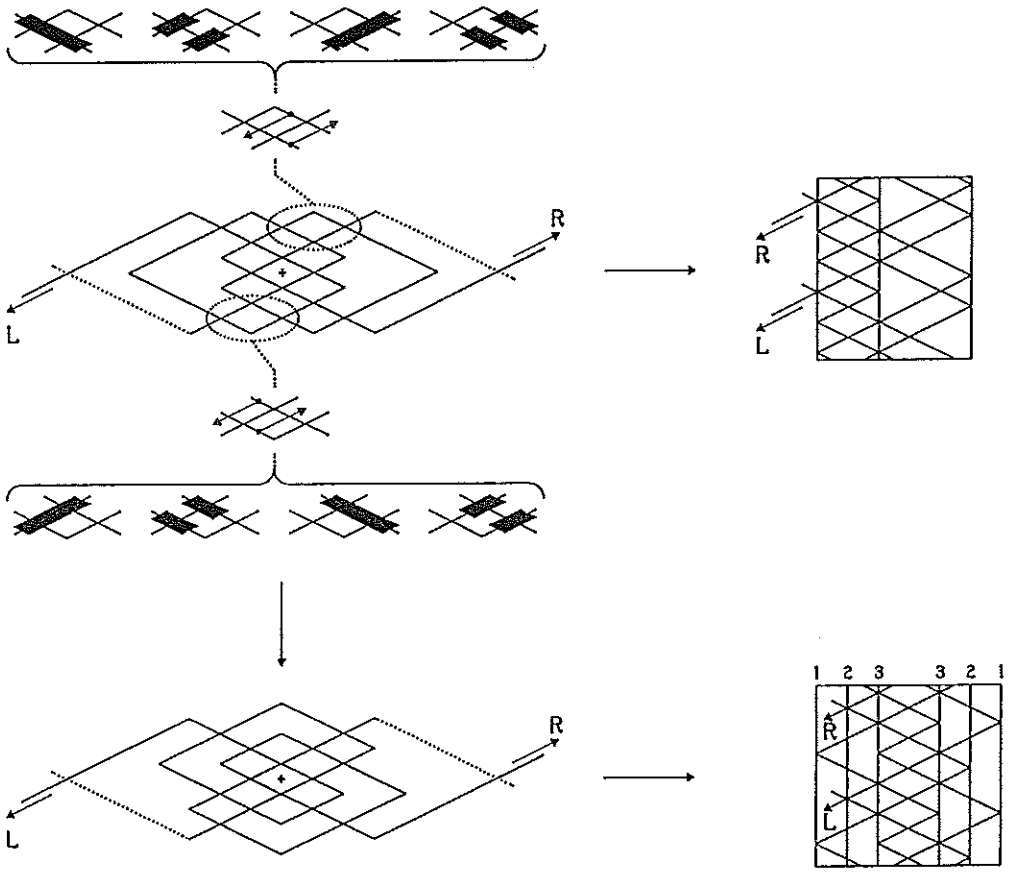

Fig. 370 — Codings which facilitate a further rearrangement of the string-run.

The necessary superimposed codings for the 'overhand' knots condition are shown in Fig. 371.

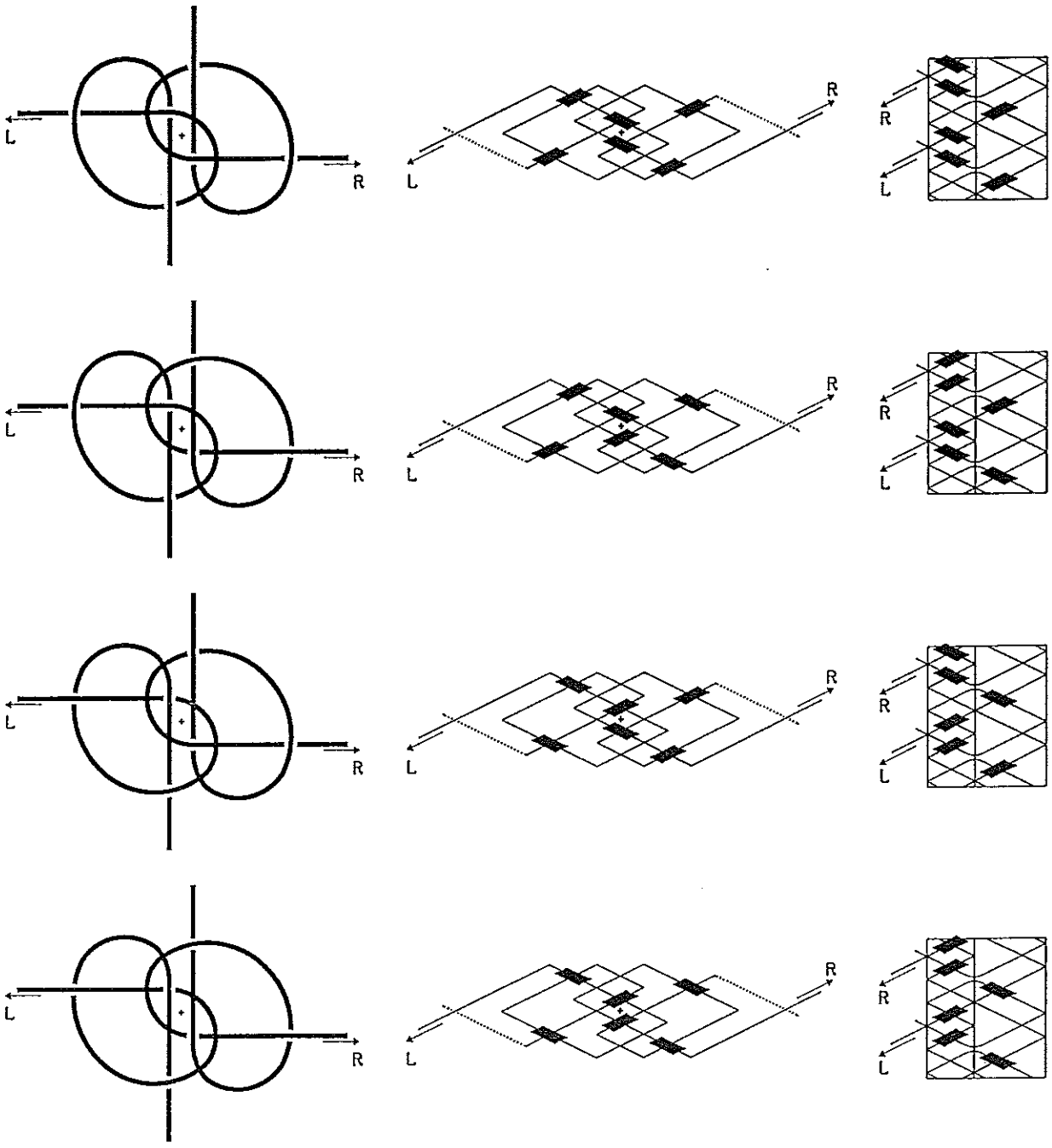

Fig. 371 — Superimposed codings for the 'overhand' knots condition.

Thus with respect to our limitations, the necessary superimposed codings for the string-runs in Fig. 368 are those depicted in Fig. 372.

In Fig. 372 the lower set of diagrams are the **everted** forms of the central set of diagrams. By comparing this lower set of diagrams with the upper set of diagrams it will be evident that they are each others **complement**.

Figs. 373&374 together show the four grid-diagrams associated with the upper layout in Fig. 372.

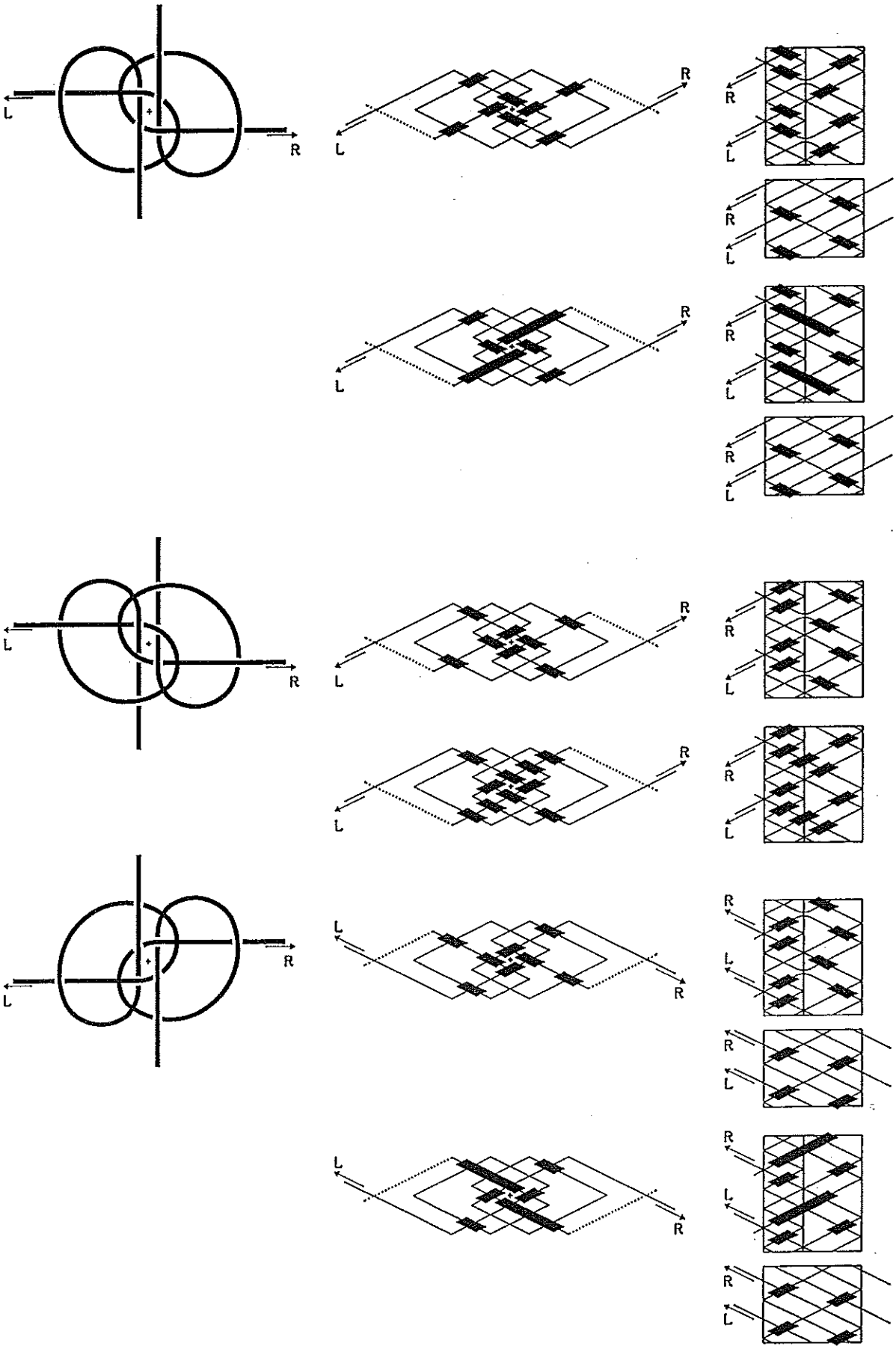

Fig.372 — The necessary superimposed codings for the string-runs in Fig. 368.

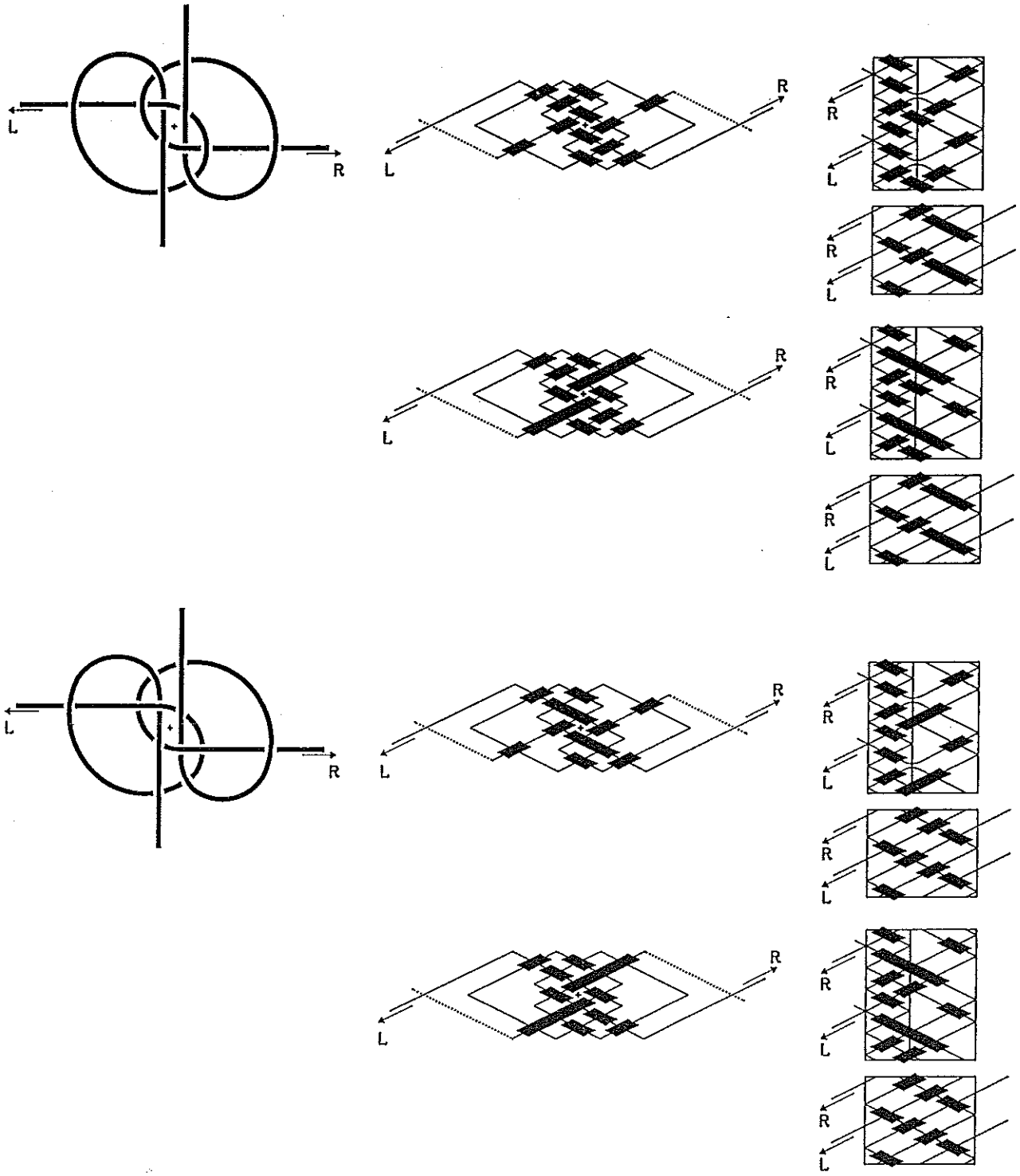

Fig. 373 — The grid-diagrams associated with the upper layout in Fig. 372.

The active ends L and R of the upper layout in Fig. 373 are the inactive ends of the lower layout in Fig. 374. The lower layout in Fig. 374 is the complement to **Ashley's Bend** (#1452 in Ashley) and the complement to **The Footrope Knot** (#783 in Ashley). By 'rolling over' the crown of the upper layout in Fig. 373 we obtain the lower layout in Fig. 374. Refer also to *The Braider*, Issue No. 5, pg. 100.

The lower layout in Fig. 373 can be rearranged in **The True-Lover's Knot** (#798 in Ashley).

The upper layout in Fig. 374 is the complement to Ashley #776 & 795 (a **Matthew Walker** open ender), which in turn is the everted form of the third layout from the top in Fig. 375.

The lower layout in Fig. 374 results in the complement to **Ashley's Bend** (#1452 in Ashley) and the complement to **The Footrope Knot** (#783 in Ashley).

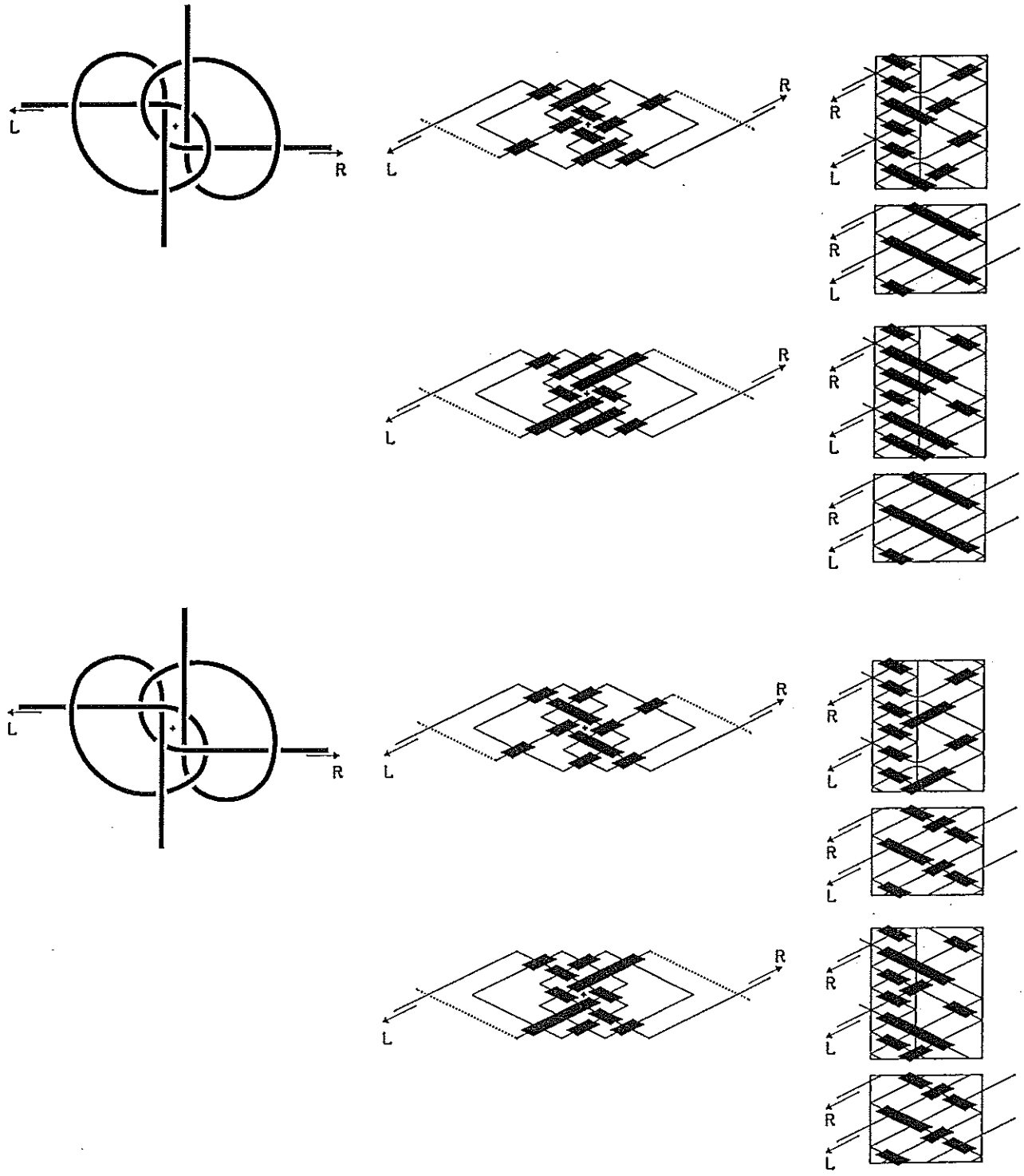

Fig. 374 — The grid-diagrams associated with the upper layout in Fig. 372.

Fig. 375 shows the four grid-diagrams associated with the central layout in Fig. 372. Figs. 376 & 377 show their everted layouts (associated with the lower layout in Fig. 372).

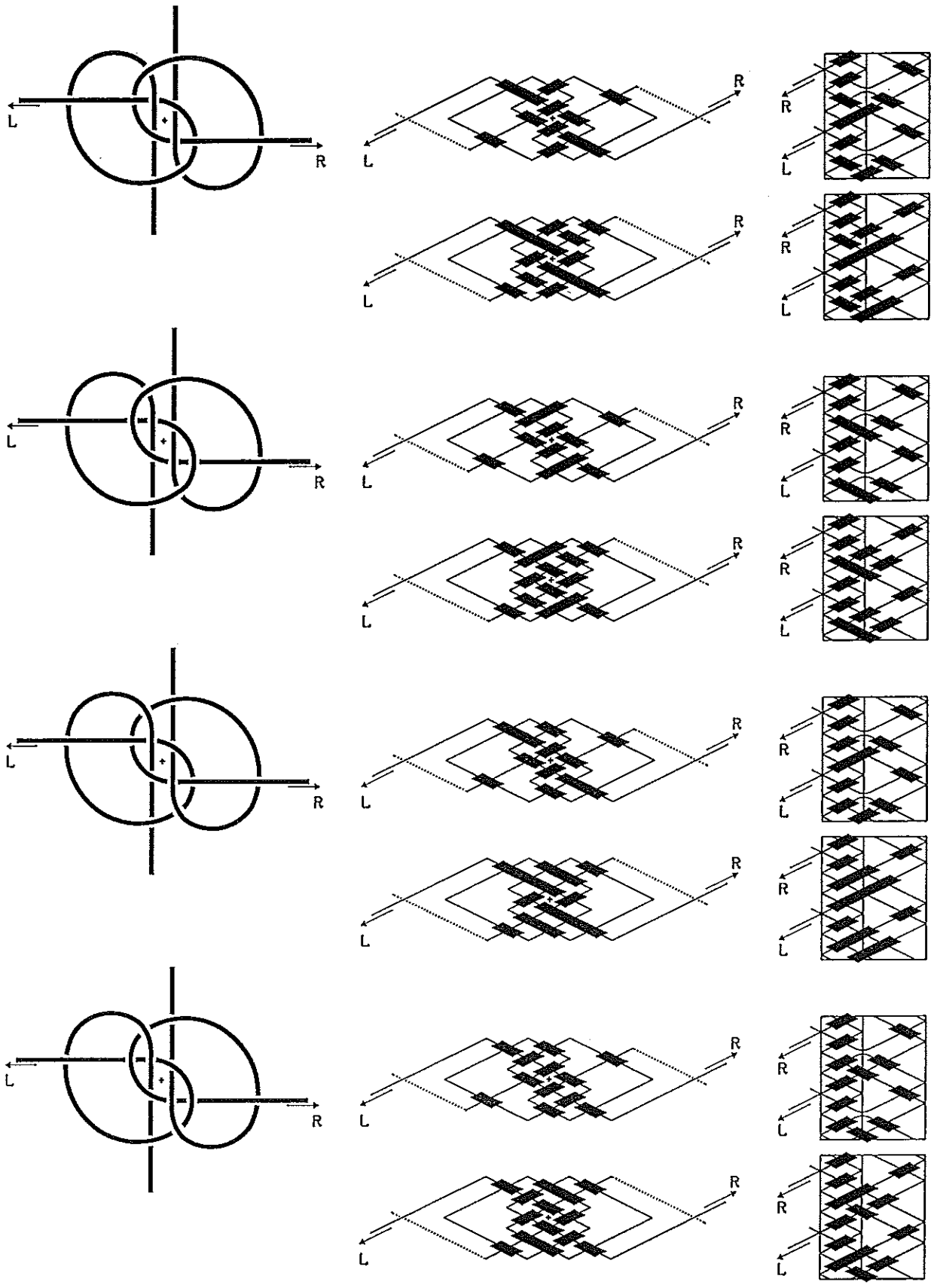

Fig. 375 — The grid-diagrams associated with the central layout in Fig. 372.

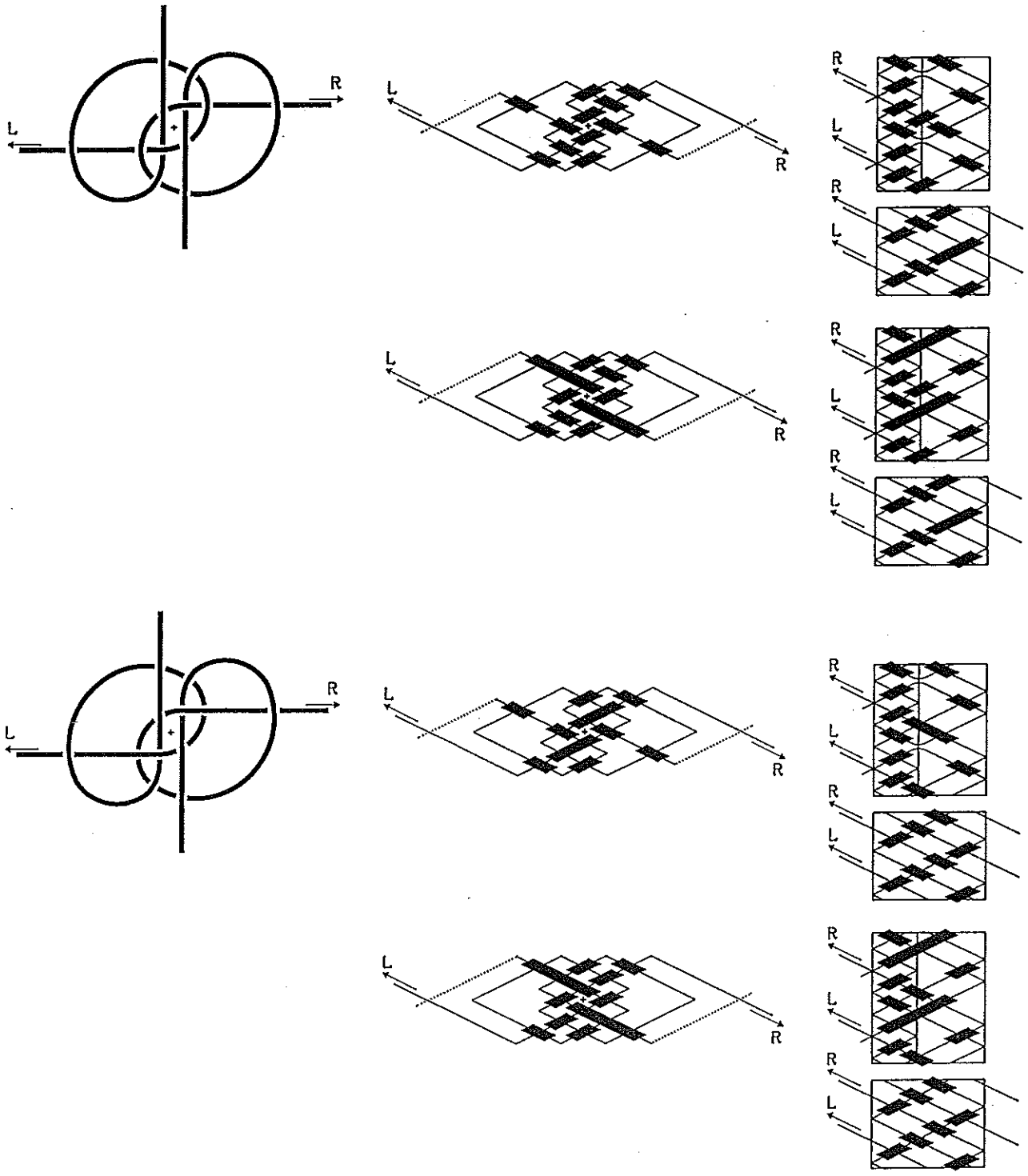

Fig. 376 — The grid-diagrams associated with the lower layout in Fig. 372.

The active ends L and R of the upper layout in Fig. 376 are the inactive ends of the lower layout in Fig. 377. The lower layout in Fig. 377 depicts **Ashley's Bend** (#1452 in Ashley) and **The Footrope Knot** (#783 in Ashley). By 'rolling over' the crown of the upper layout in Fig. 376 we obtain the lower layout in Fig. 377. Refer also to *The Braider*, Issue No. 5, pg. 100. The upper layout in Fig. 376 is the complement of the upper layout in Fig. 373.

The lower layout in Fig. 376 can be rearranged to the complement of **The True-**

Lover's Knot (the complement to#798 in Ashley). The lower layout in Fig. 376 is the complement to the lower layout in Fig. 373.

The upper layout in Fig. 377 depicts #776 & 795 in Ashley (a **Matthew Walker** open ender). The upper layout in Fig. 377 is the complement of the upper layout in Fig. 374.

The lower layout in Fig. 377 depicts **Ashley's Bend** (#1452 in Ashley) and **The Footrope Knot** (#783 in Ashley). The lower layout in Fig. 377 is the complement to the lower layout in Fig. 374.

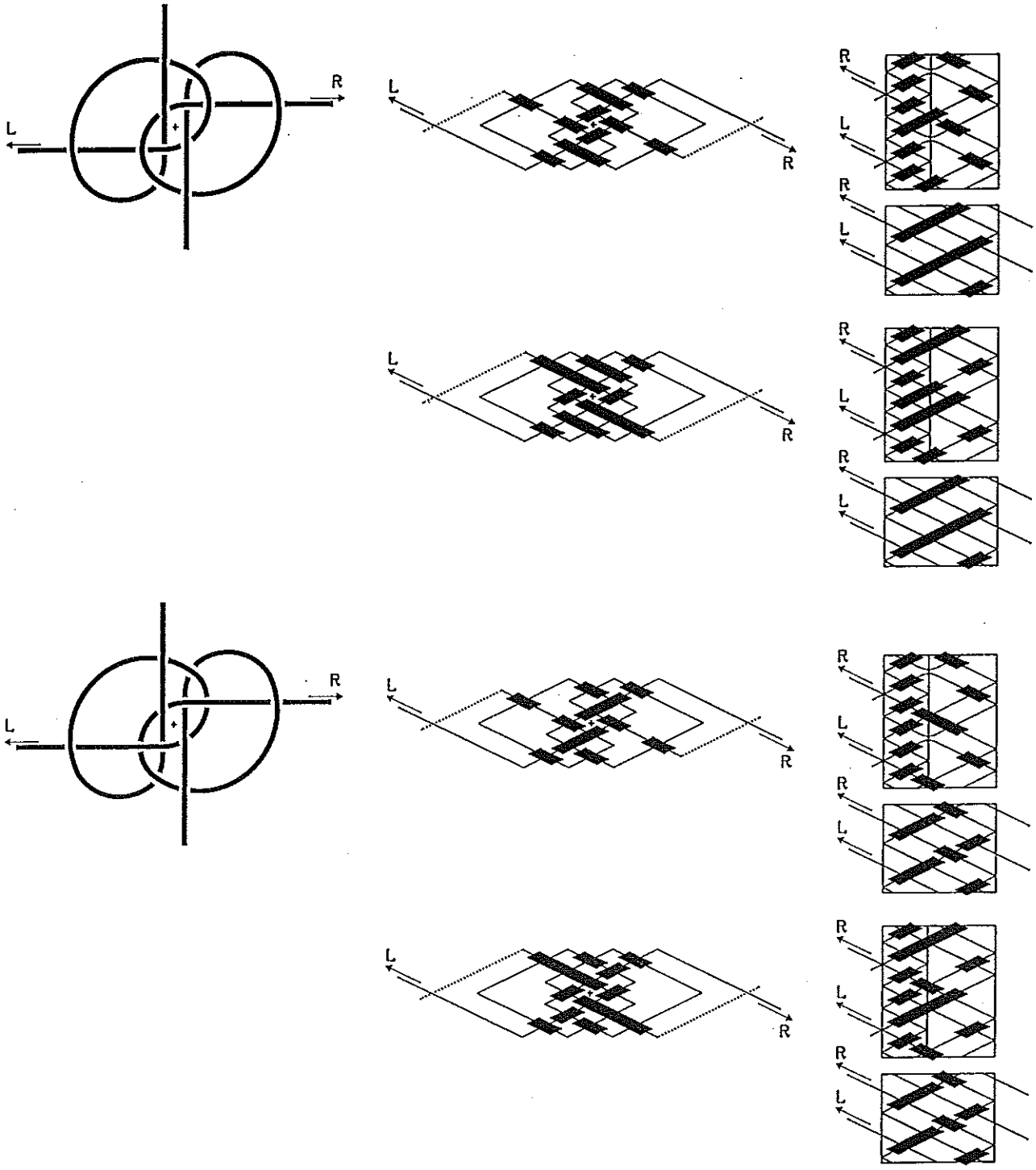

Fig. 377 — The grid-diagrams associated with the lower layout in Fig. 372.

In the previous Figs. 373–377 as well as in the following Figs. 379–381 the crossing-sequences from the ends L and R are identical for the coding arrangements of the two interbraided strings. These two sets of figures form however, with respect to the types of grid-diagram shown, two distinct categories.

The first layout in Fig. 379 depicts **Hunter's Bend** (#1425*A* in Ashley).

The second layout in Fig. 379 results in the left-hand string configuration of Fig. 378.

The third layout in Fig. 379 depicts #1425 in Ashley. This is an excellent bend for flat string.

The final layout in Fig. 379 results in the right-hand string configuration of Fig. 378.

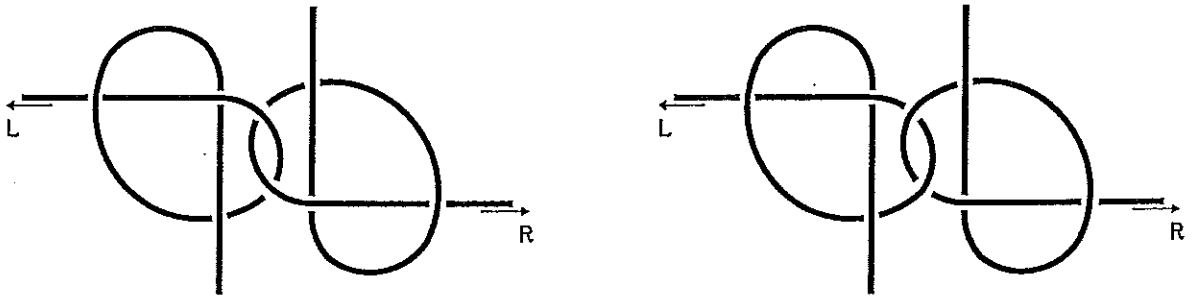

Fig. 378 — The rearranged layouts for the second and fourth layout in Fig. 379.

The everted forms of the layouts in Fig. 380 are depicted in Fig. 381. These everted forms are respectively the complements of the forms in Fig. 379.

Since we are limiting our discussion to braiding material which is symmetric with respect to shape, colour and pattern/texture, we need to concern ourselves only with the various balanced superimposed coding arrangements associated with the second layout from the top in Fig. 371 (note that with these limitations the third layout from the top in Fig. 371 is **lateral equivalent**† to the second layout from the top).

We thus have to investigate the eight balanced coding arrangements which are associated with the second layout from the top in Fig. 371. These arrangements are shown in Figs. 382 & 385.

The crossing-sequences from the ends L and R, associated with these coding arrangements, are opposites for each of the two interbraided strings.

The uppermost layout in Fig. 382 depicts **The Zeppelin Bend.**

The two components in the second and third layout from the top in Fig. 382 slide apart.

The lowermost layout in Fig. 382 can be rearranged into the central layout shown in Fig. 383. Although this rearrangement is called in *The Century Guide to Knots*, by Mario Bigon and Guido Regazzoni, pp. 138 & 139, **The Water Knot**‡, **The Fisherman's Knot**, **The English Knot**, **The Englishman's Knot**, **The True-Lover's Knot**, **The Angler's Knot**, it is quite a different knot to the one by the same names in Ashley (#496 & #1414). The Waterman's Knot in Ashley has been depicted in Fig. 384. Although the string-run of the knot in Fig. 383 can be rearranged into the lowermost string-runs shown in Fig. 383, hence to the type of string-runs shown for the knot in Ashley (Fig. 384), the knot in Ashley (Fig. 384) cannot be rearranged into the type of

† Refer for more details to Pamphlet No. 8: *Knots — Facts and Fallacies.*

‡ Note that the name **Water Knot** is used for various knots (see Ashley #296, #343, #1412, #1414). The name **Waterman's Knot** should here be preferred instead (see Ashley #1414).

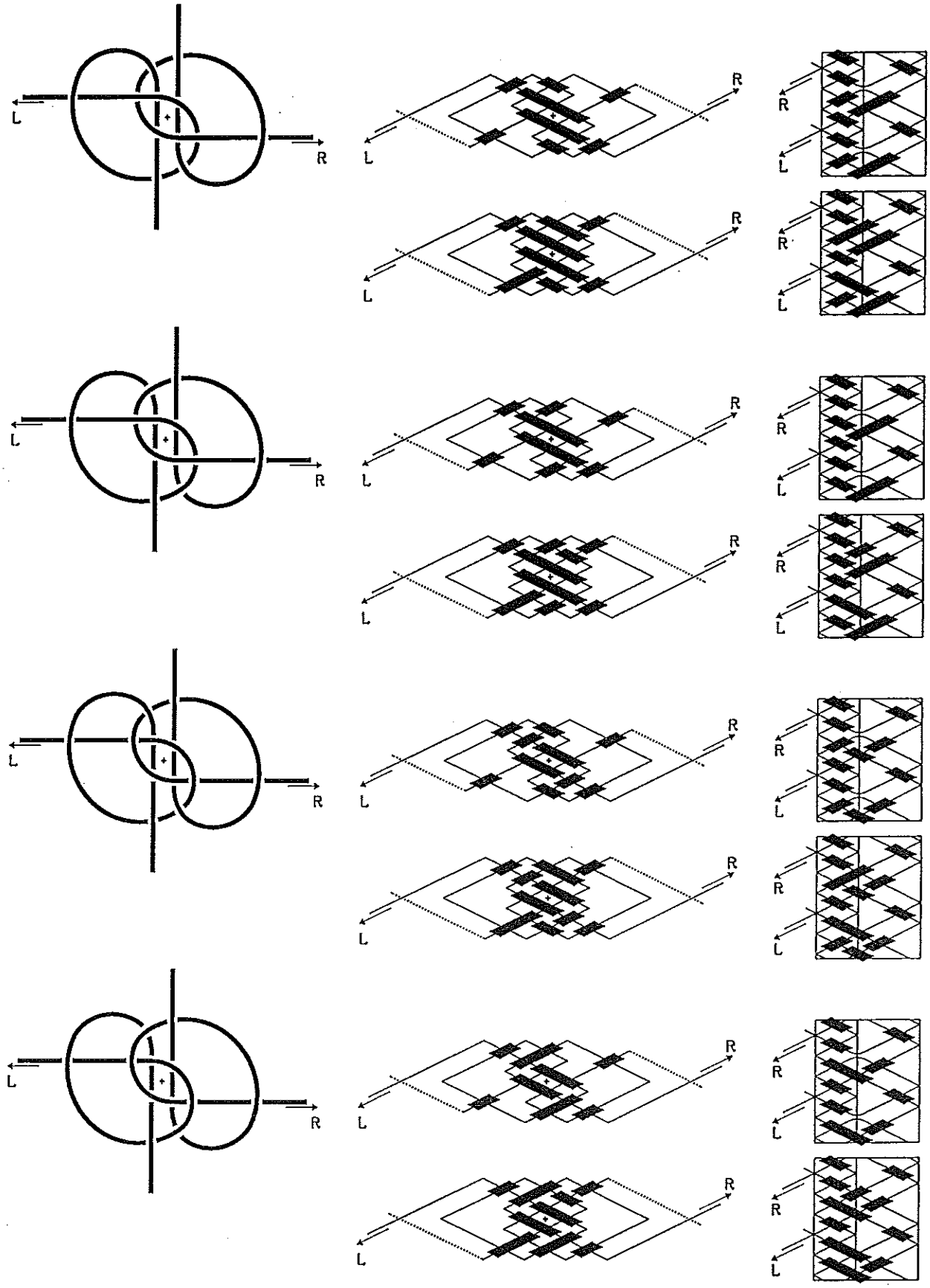

Fig. 379 — Further layouts with identical crossing-sequences for the two components.

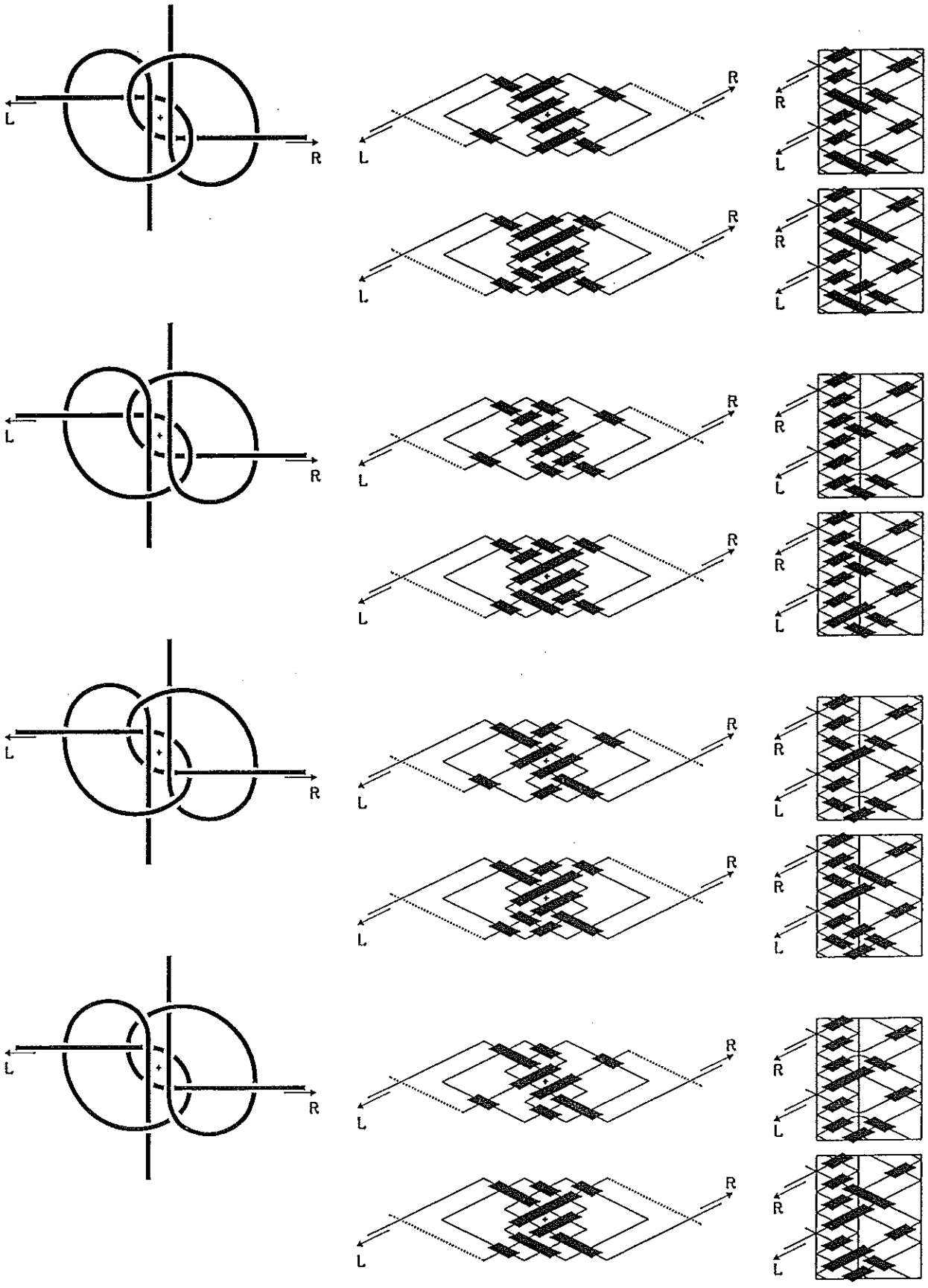

Fig. 380 — Further layouts with identical crossing-sequences for the two components.

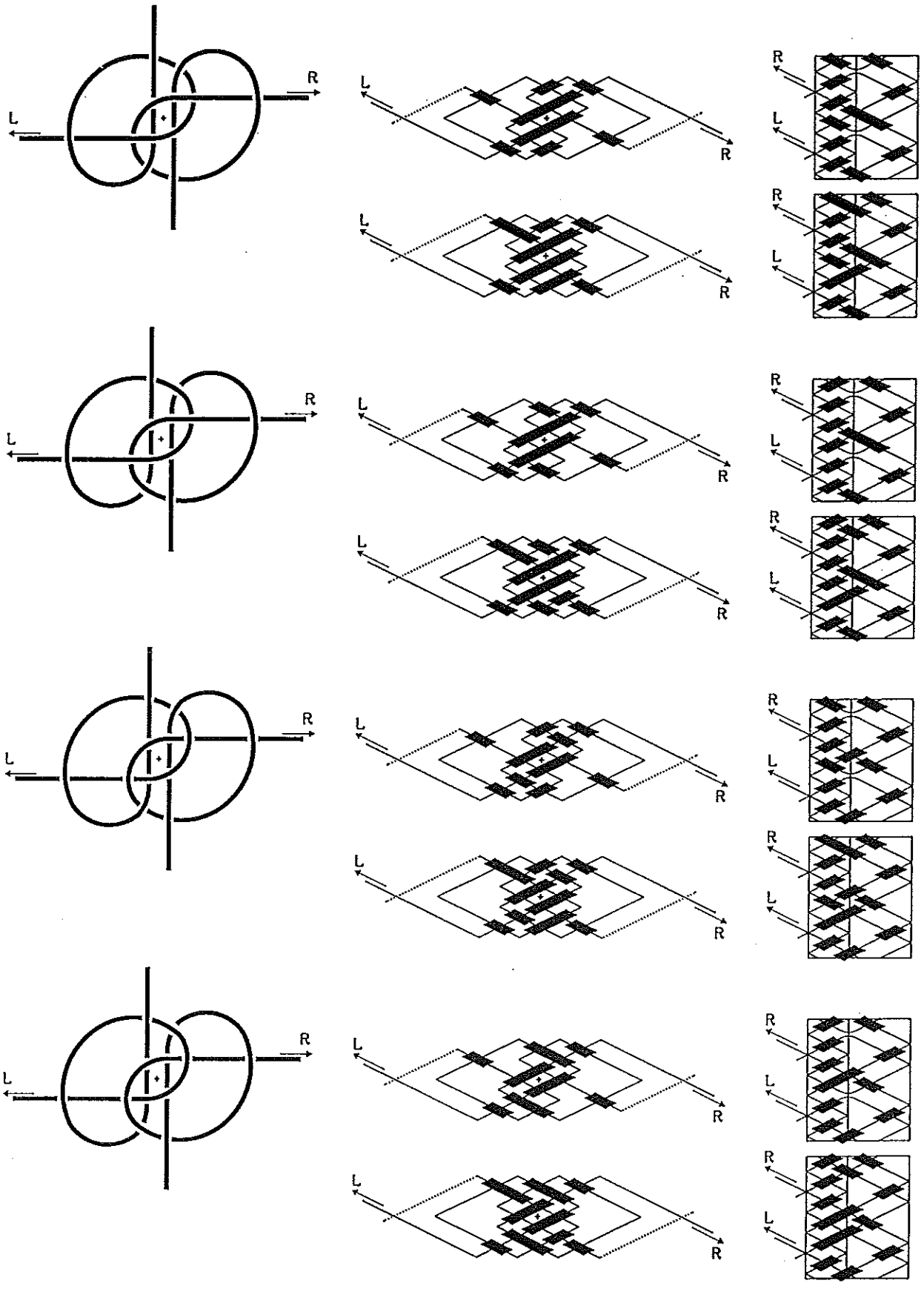

Fig. 381 — The everted forms of the layouts in Fig. 380.

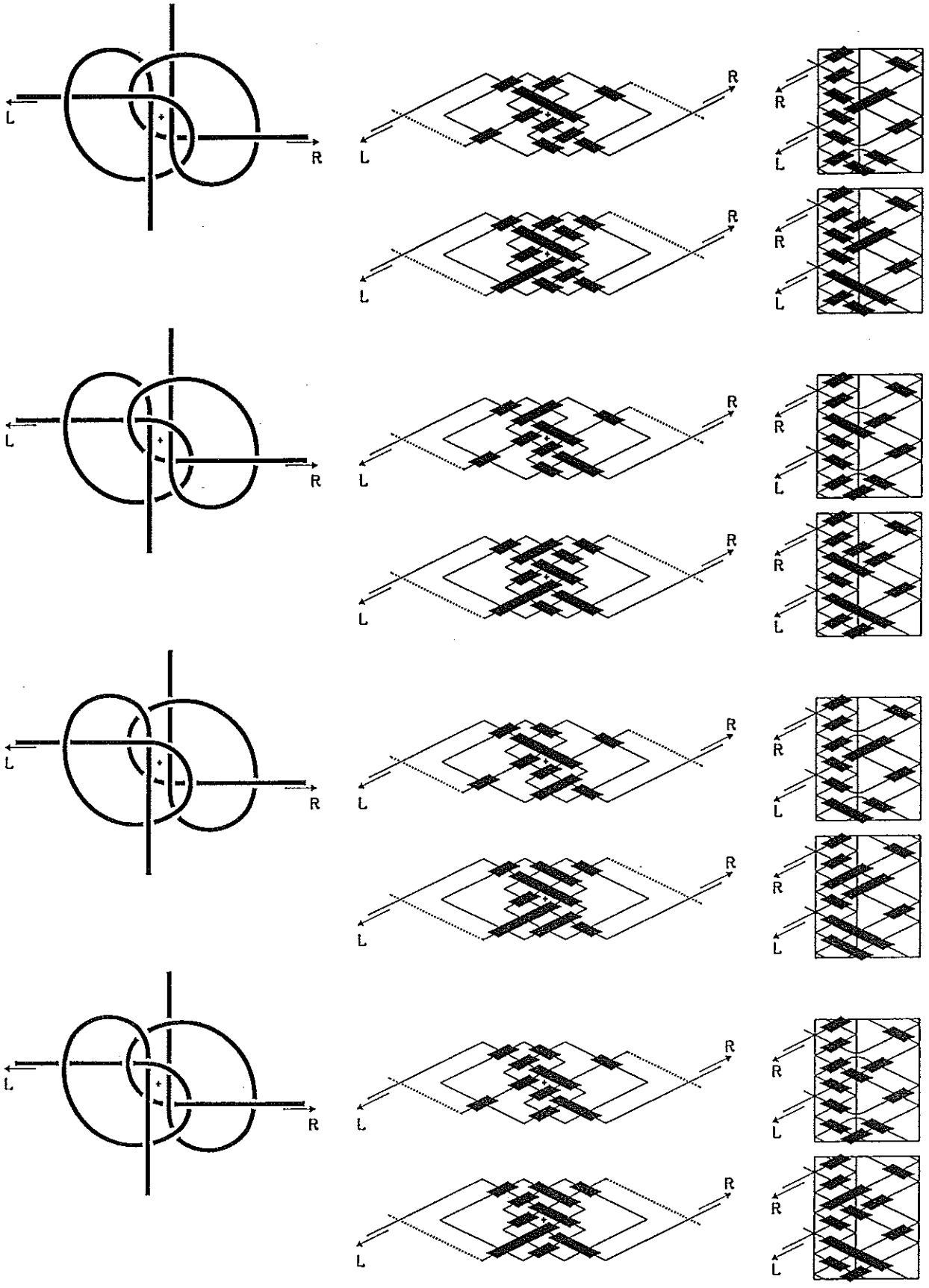

Fig. 382 — Layouts with opposites as crossing-sequences for the two components.

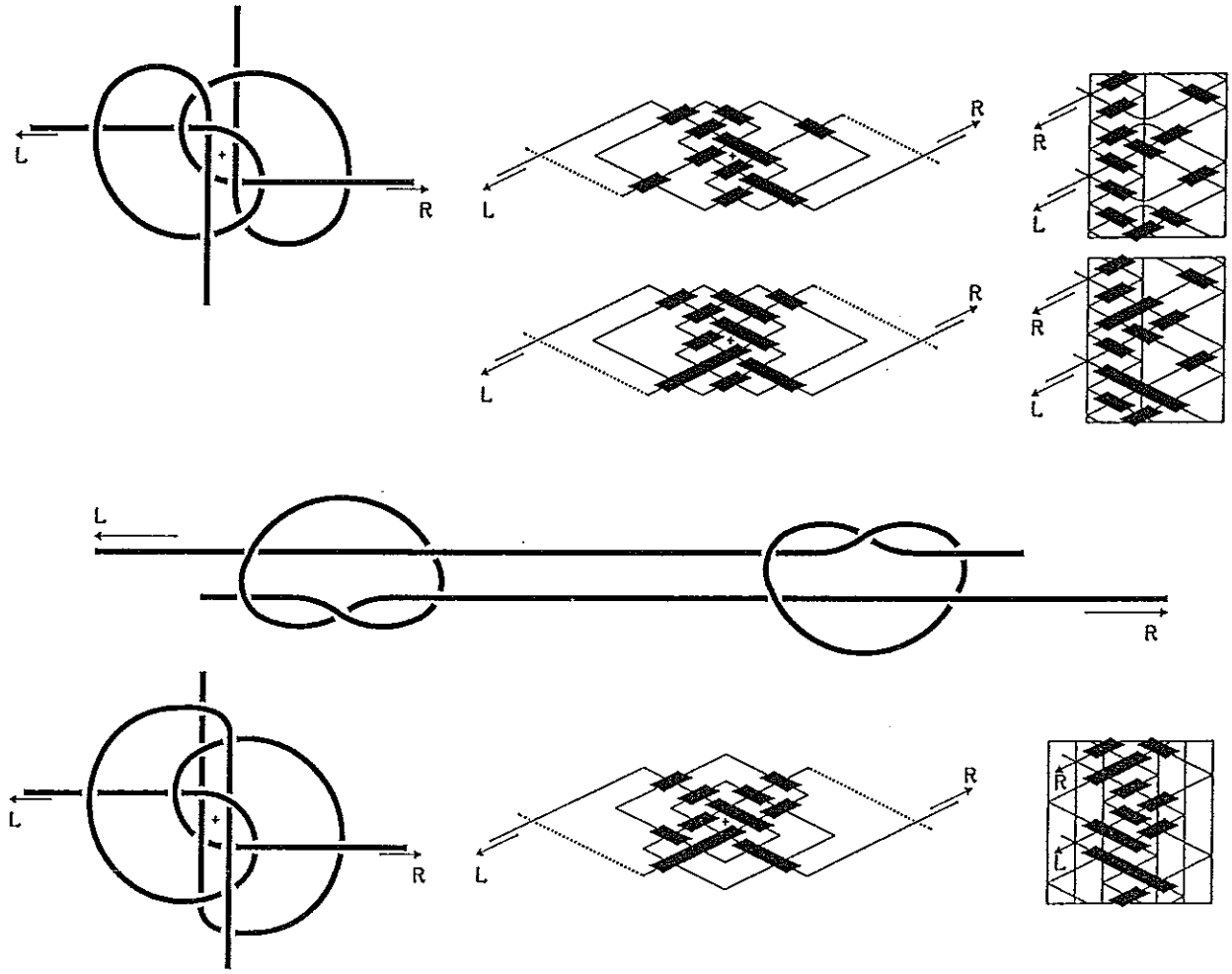

Fig. 383 — The lowermost layout in Fig. 382.

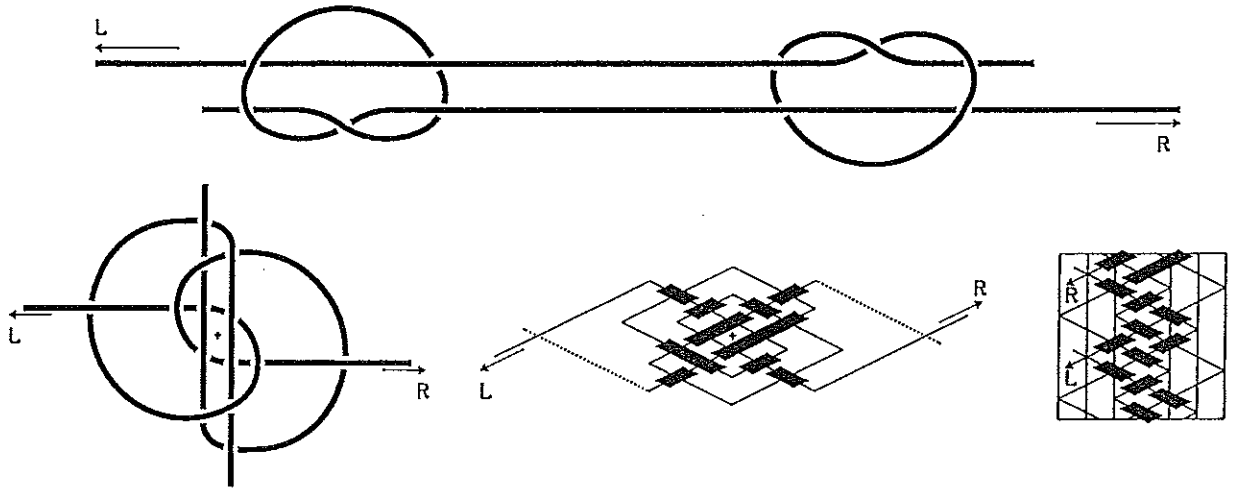

Fig. 384 — The Waterman's Knot #496 & #1414 in Ashley.

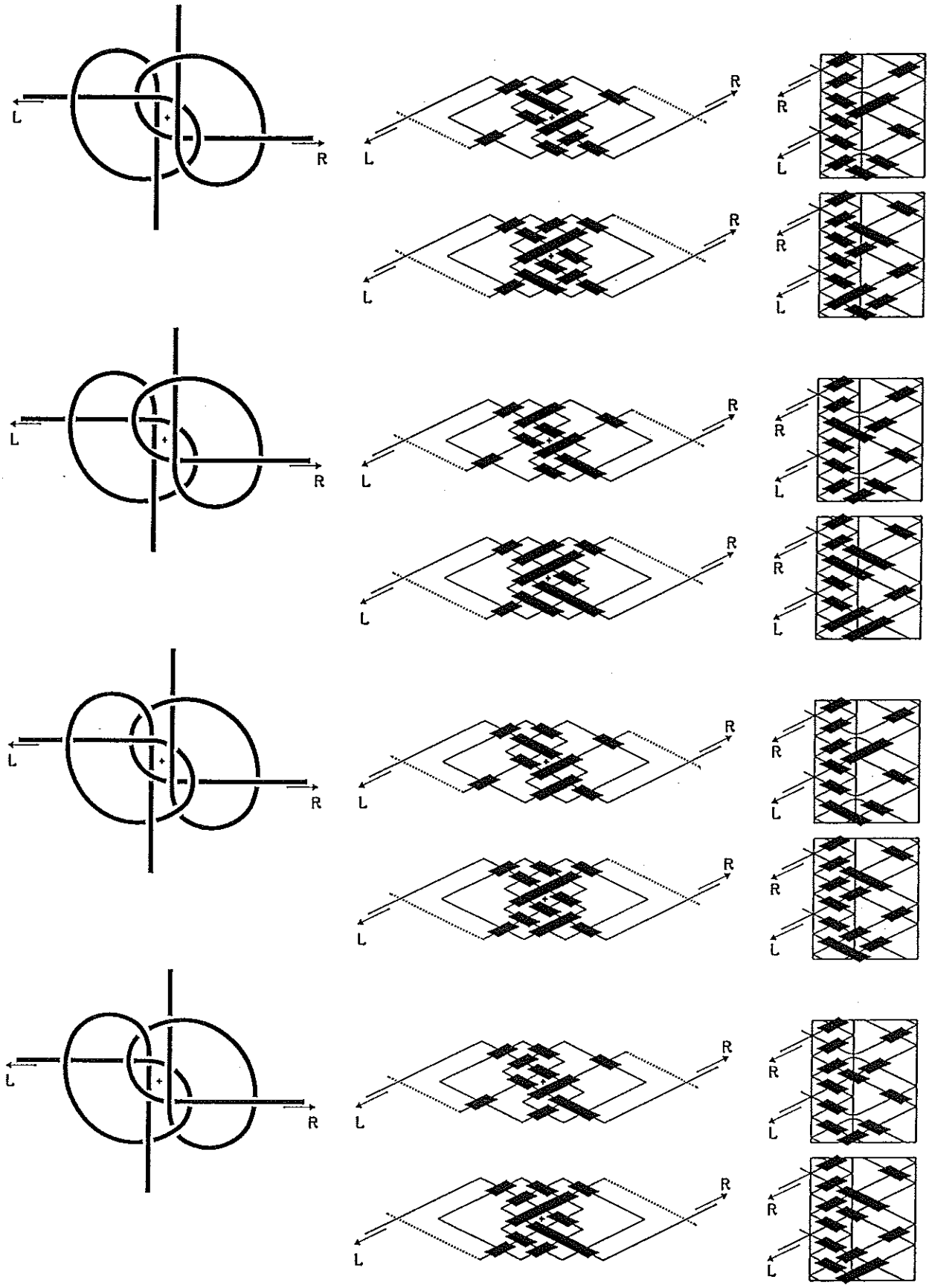

Fig. 385 — Layouts with opposites as crossing-sequences for the two components.

string-runs shown in the upper part of Fig. 383 (refer to pg. 447). Hence, notwithstanding that the Waterman's Knots knots in Ashley and in *The Century Guide to Knots* appear superficially similar, they are quite different. It should be noted that the Waterman's Knot in Ashley has in the rearrangements shown in Fig. 384 **not** a balanced coding, whereas the Waterman's Knot in *The Century Guide to Knots*, shown in Fig. 383, does have a balanced coding. However, the Waterman's Knot in Ashley which does have a balanced coding in the upper string-run of Fig. 384 ([L: $u-2o-u-2o-2u-o-u.$] and [R: $u-2o-u-2o-2u-o-u.$]) is a considerably better knot than the Waterman's Knot in *The Century Guide to Knots*, which also has a balanced coding in the central string-run of Fig. 383 ([L: $u-o-u-o-2u-2o-u-o.$] and [R: $o-u-o-u-2o-2u-o-u.$]).

The first two layouts in Fig. 385 are rearrangements of each other and the two components can be slid apart.

The last two layouts in Fig. 385 are also rearrangements of each other. The active ends L and R of these two layouts are the inactive ends of the everted Zeppelin Bend, the everted upper layout in Fig. 382.

This very limited discussion involving a rather simple string run layout should clearly demonstrate the complications which are an inherent part of any classification attempt for knots and braids.

The Zeppelin Bend is also called the Rosendahl Bend by Geoffrey Budworth (*The Knot Book, pg. 129*), and is called the Rosenthal Bend by Brion Toss (*The Rigger's Apprentice, pg. 47*). Who can solve the question who of the two got it right, hence whether it should be Rosendahl Bend or Rosenthal Bend.

In *The Australian Whipmaker*, No. 44, pg. 838, a knot has been depicted by Ron Edwards to whom it was shown by a visitor who apparently called it 'Hunter's Knot'. However, this knot is **not** Hunter's Bend as the leftmost layout in Fig. 386 readily shows. In order to avoid any confusion we shall call this knot here '**The Edwards' Knot**'.

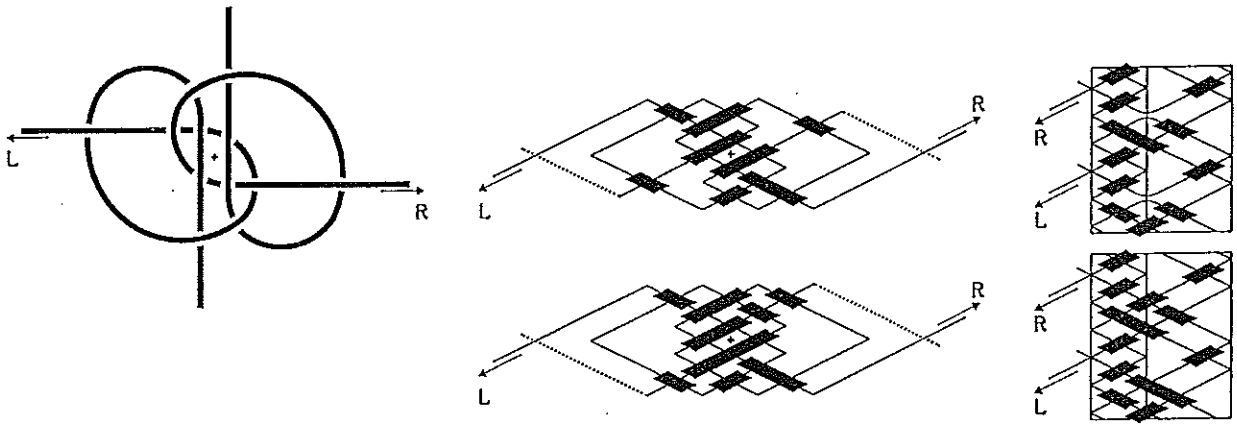

Fig. 386 — The Edwards' Knot.

It should be observed that this knot does not have a balanced coding. It differs in one crossing from the uppermost layout in Fig. 380, or its string-run can be rearranged so that it differs in one crossing (at the same crossing-point) from the third layout in Fig. 380. This knot undoubtedly resulted from erroneously tying Hunter's Bend.